

Accepted Manuscript

Discovery of novel vinyl sulfone derivatives as anti-tumor agents with microtubule polymerization inhibitory and vascular disrupting activities

Wenlong Li, Ying Yin, Hong Yao, Wen Shuai, Honghao Sun, Shengtao Xu, Jie Liu, Hequan Yao, Zheyang Zhu, Jinyi Xu



PII: S0223-5234(18)30746-3

DOI: [10.1016/j.ejmech.2018.08.074](https://doi.org/10.1016/j.ejmech.2018.08.074)

Reference: EJMECH 10685

To appear in: *European Journal of Medicinal Chemistry*

Received Date: 19 April 2018

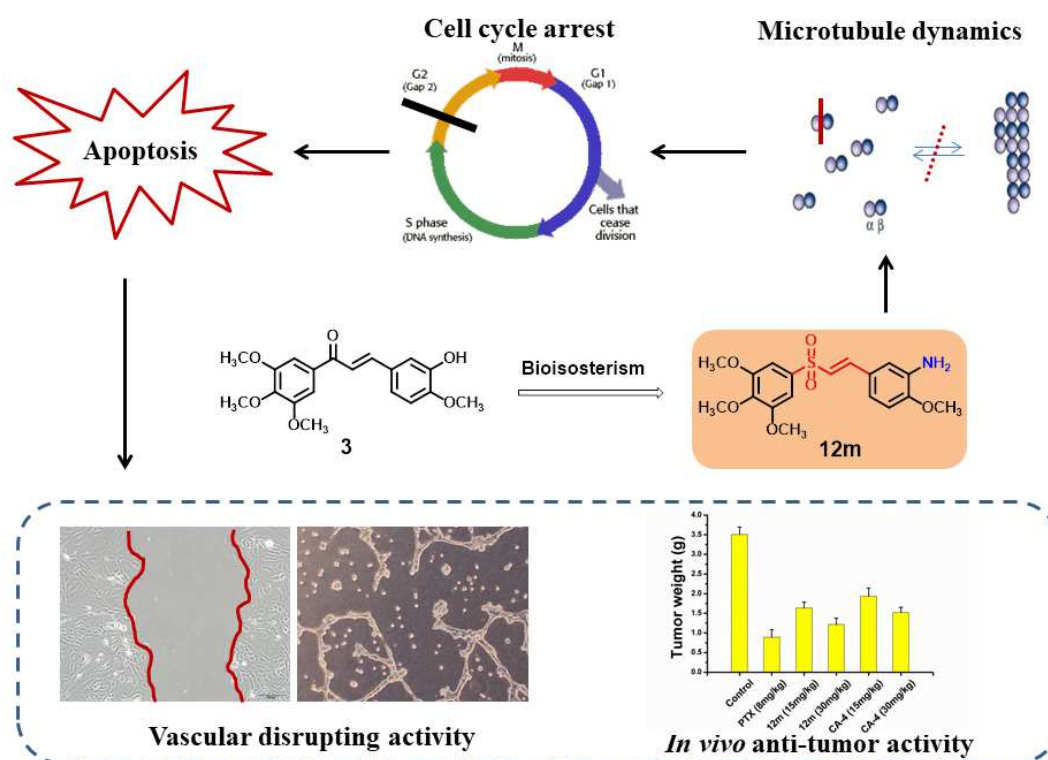
Revised Date: 7 August 2018

Accepted Date: 26 August 2018

Please cite this article as: W. Li, Y. Yin, H. Yao, W. Shuai, H. Sun, S. Xu, J. Liu, H. Yao, Z. Zhu, J. Xu, Discovery of novel vinyl sulfone derivatives as anti-tumor agents with microtubule polymerization inhibitory and vascular disrupting activities, *European Journal of Medicinal Chemistry* (2018), doi: 10.1016/j.ejmech.2018.08.074.

This is a PDF file of an unedited manuscript that has been accepted for publication. As a service to our customers we are providing this early version of the manuscript. The manuscript will undergo copyediting, typesetting, and review of the resulting proof before it is published in its final form. Please note that during the production process errors may be discovered which could affect the content, and all legal disclaimers that apply to the journal pertain.

Graphic abstract



ACCEPTED MANUSCRIPT

Discovery of Novel Vinyl Sulfone Derivatives as Anti-tumor Agents with Microtubule Polymerization Inhibitory and Vascular Disrupting Activities

Wenlong Li^a, Ying Yin^a, Hong Yao^a, Wen Shuai^a, Honghao Sun^a, Shengtao Xu^{a,*}, Jie Liu^{b,c}, Hequan Yao^a, Zheyang Zhu^d, Jinyi Xu^{a,*}

^a State Key Laboratory of Natural Medicines and Department of Medicinal Chemistry, China Pharmaceutical University, 24 Tong Jia Xiang, Nanjing 210009, P. R. China

^b Department of Organic Chemistry, China Pharmaceutical University, 24 Tong Jia Xiang, Nanjing 210009, P. R. China

^c State Key Laboratory for the Chemistry and Molecular Engineering of Medicinal Resources, and School of Chemistry and Pharmacy, Guangxi Normal University, Guilin 541004, China

^d Division of Molecular Therapeutics & Formulation, School of Pharmacy, The University of Nottingham, University Park Campus, Nottingham NG7 2RD, UK

*Corresponding Author:

E-mail addresses: cpuxst@163.com (S. Xu), jinyixu@china.com (J. Xu).

Abstract

Vinyl sulfone or sulfoxide moieties were firstly introduced to the structure of chalcone compound by replacing the carbonyl group to afford a series of novel compounds as potential anti-tubulin agents. All of the target compounds were evaluated for their anti-proliferative activity. Among them, compound **12m** showed the most potent activity against a panel of cancer cell lines with IC₅₀ values ranging from 0.128 to 0.606 μ M. Further mechanism studies demonstrated that compound **12m** caused G2/M phase arrest, induced cell apoptosis and disrupted the intracellular microtubule network. Moreover, compound **12m** reduced the cell migration and disrupted the capillary-like tube formation in human umbilical vein endothelial cell (HUVEC) assays. Importantly, compound **12m** significantly and dose dependently inhibited tumor growth in H22 liver cancer allograft mouse model, which is more potent than control compound CA-4, suggesting that **12m** deserves further research as

a potential anti-tubulin agent targeting colchicine binding site on tubulin.

Key words: tubulin inhibitors; vinyl sulfone; colchicine binding site; anti-tumor activity

1. Introduction

Microtubules are formed by the lateral aggregation of protofilaments, each of which is composed of a chain of stable α - and β -tubulin dimers [1]. They are not simple equilibrium polymers, instead they show complex polymerization dynamics which are crucial to their cellular functions. The vital roles in cell proliferation, trafficking, signaling and migration in eukaryotic cells make microtubules an important target for cancer therapy [2]. Microtubule targeting agents (MTAs) that bind to the taxane or vinca alkaloid binding site on tubulin, such as paclitaxel and vinblastine, have been widely used in clinic for the treatment of cancers [3]. However, the extremely structural complexity, low aqueous solubility as well as multidrug resistance (MDR) and dose-limiting toxicity of these taxane and vinca alkaloid binding sites inhibitors hampered their clinical applications. Nevertheless, MTAs that target colchicine binding site on tubulin are generally characterized with simpler skeletons, such as colchicine (**1**), combretastatin A-4 (**2**, CA-4) and their analogues **3** and **4** (Fig.1), which have the potential to overcome these limitations. Interest in these colchicine binding site inhibitors (CBSIs) has been further raised by the discovery that tubulin inhibitors especially those bind at colchicine binding site can target existing vessels in the tumor tissues, thereby provoking a rapid collapse of the tumor vasculature [4, 5]. Thus, CBSIs endowed with both antimitotic and vascular disrupting profiles are continuing to attract pharmaceutical interest [6-8], which provides a novel promising treatment for cancer therapy.

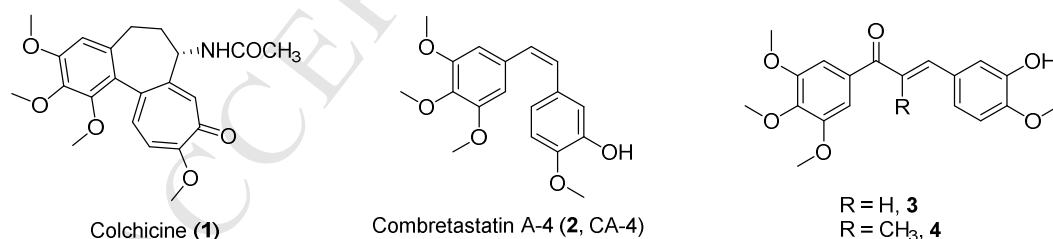


Fig. 1. Structures of the representative tubulin polymerization inhibitors and vascular disrupting agents (VDAs).

In our prior review about the privileged structures of CBSIs, α,β -unsaturated ketone structure that is mostly found in chalcones was considered as a privileged bridge in the development of CBSIs [9]. Representative anti-tubulin chalcones are compound **3** and **4** which were reported by Ducki's group in 1998, both showed remarkable anti-proliferative activities [10]. The introduction of methyl on α position of carbonyl

led to a dramatically improved cytotoxicity due to the more preferential *s-trans* conformation adopted by **4**, while *s-cis* conformation by **3** led to less potent activity. Comprehensive structure-activity relationships (SARs) studies were conducted with a conclusion that compound **4** bearing 2-methyl substituted α,β -unsaturated ketone as the bridge was the most active [11, 12].

Vinyl sulfone has long been known for their synthetic utility in organic chemistry, easily participating in 1,4-addition reactions and cycloaddition reactions [13]. Recently, this moiety has also been shown to exhibit a wide range of biological activities including cysteine protease inhibition [14], neuroprotection [15, 16], c-FLIP inhibition [17] and anti-tumor effects [18-20]. Thus, inspired by the structural similarity of vinyl sulfone or sulfoxide to vinyl carbonyl as Michael acceptors, we introduced vinyl sulfone or sulfoxide moieties to the structure of compound **3** to afford a series of novel compounds as potential anti-tubulin agents (Fig. 2). Considering the vital effect of methyl substituted at α position of α,β -unsaturated ketone of compound **4**, various groups were introduced to the α position of vinyl sulfones or sulfoxides to explore the SARs. Herein, we report the synthesis, *in vitro* and *in vivo* anti-tumor activity and mechanism studies of a series of novel vinyl sulfone and sulfoxide derivatives as anti-tubulin agents targeting colchicine binding site on tubulin.

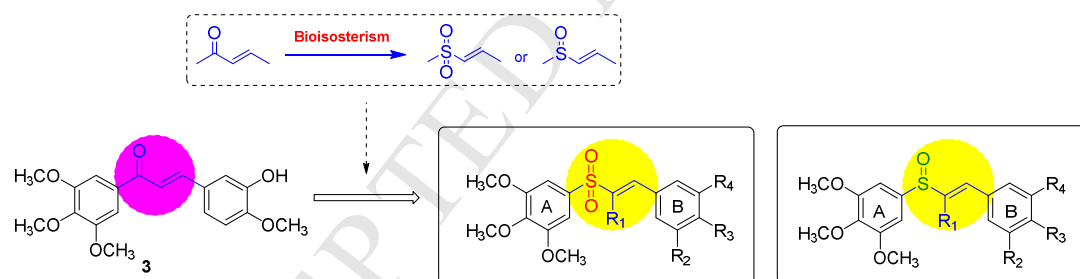


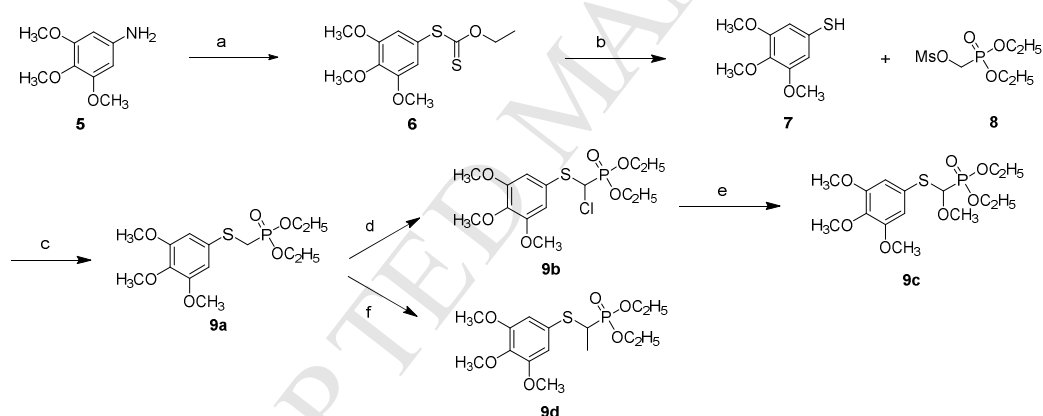
Fig. 2. The design of vinyl sulfone and sulfoxide derivatives as tubulin inhibitors.

2. Results and discussion

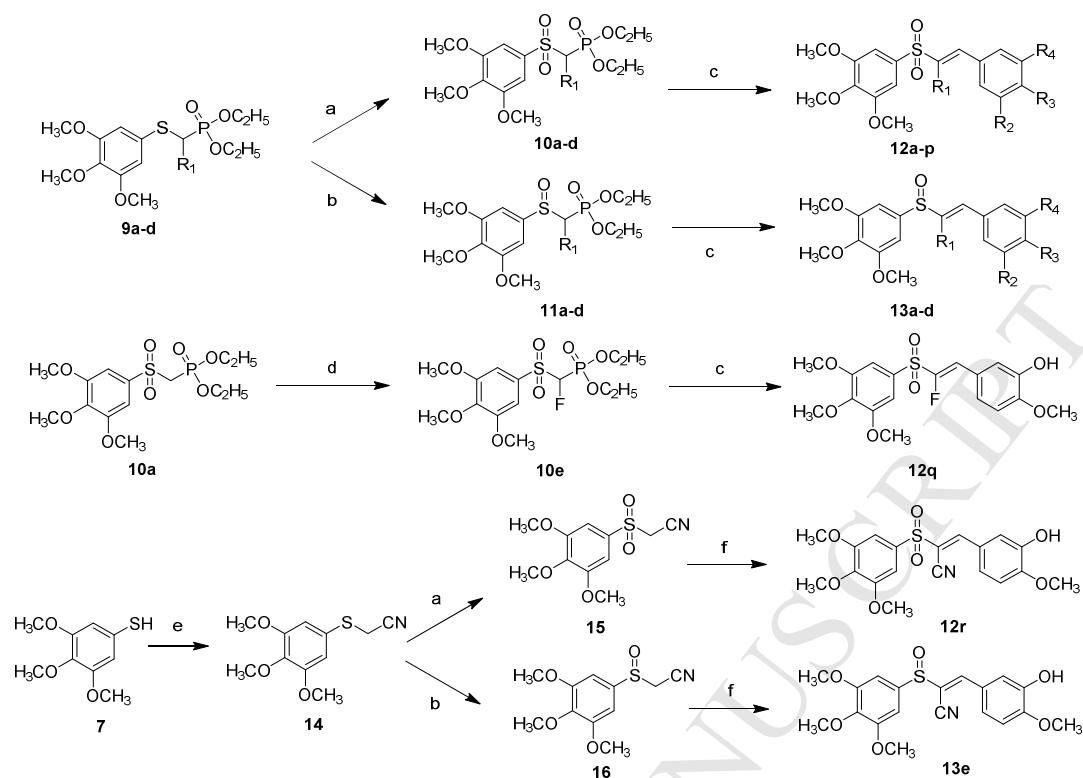
2.1 Chemistry

The synthetic routes for the vinyl sulfones and sulfoxides are outlined in Schemes 1-2. Intermediate 3,4,5-trimethoxybenzothiol **7** was prepared by diazo reaction of commercially available 3,4,5-trimethoxyaniline with potassium ethyl xanthate, following hydrolyzation under basic conditions. The key intermediate phosphate **9a** was obtained by a nucleophilic reaction of **7** with diethoxyphosphorylmethyl 4-methylbenzenesulfonate **8** in the presence of K₂CO₃ in acetonitrile. Subsequently, various groups were introduced to the α position of phosphonate, chlorine-substituted **9b** was afforded by treating **9a** with *N*-chlorine

succinimide (NCS) in carbon tetrachloride, and **9b** was further converted to **9c** in refluxing methanol. Deprotonation of α -proton of phosphonate in **9a** was carried out by using *n*-butyllithium in THF under -78°C , and the resulting carbanion was reacted with methyl iodide to give **9d**. Then phosphonates **9a-d** were further selectively oxidized to afford corresponding sulfones **10a-d** and sulfoxides **11a-d** by controlling the equivalents of *m*-chloroperbenzoic acid (*m*-CPBA). Fluoro-substituted sulfone **10e** was obtained by treating **10a** with NaH and equivalent selectfluor in THF. Finally, all prepared phosphonates with sulfone or sulfoxide group were undergone Wittig-horner reactions with various aromatic aldehydes to produce the corresponding vinyl sulfones **12a-q** and vinyl sulfoxides **13a-d**. Cyan-substituted vinyl sulfone **12r** and vinyl sulfoxide **13e** were synthesized through another route. Intermediate **7** was reacted with bromoacetonitrile under basic condition, and the furnished **14** was oxidized to sulfone **15** and sulfoxide **16**, which were further undergone Knoevenagel reactions with acetyl protected isovanillin, and further deprotection of acetyl group produced target vinyl sulfone **12r** and vinyl sulfoxide **13e**, respectively. Altogether, twenty three compounds were finally synthesized as shown in Fig. 3.



Scheme 1. Reagents and conditions: (a) (i) NaNO_2 , 10% HCl , CH_3OH , 0°C ; (ii) potassium ethyl xanthate, 65°C , 55%; (b) 10% NaOH , CH_3OH , rt, 94%; (c) K_2CO_3 , CH_3CN , rt, 63%; (d) NCS, CCl_4 , rt, 72%; (e) CH_3OH , reflux, 90%; (f) (i) *n*-BuLi, THF, -78°C ; (ii) CH_3I , -78°C - 45°C , 48%.



Scheme 2. Reagents and conditions: (a) *m*-CPBA (2.2 e.q), DCM, rt, 55-90%; (b) *m*-CPBA (0.9 e.q), DCM, 0°C, 58-82%; (c) NaH, acetyl protected aldehydes, THF, N₂, 0°C; when R₃ or R₄ = OH (i) NaH, aldehydes, THF, N₂, 0°C; (i) 10% NaOH, CH₃OH, rt, 28-87%; (d) NaH, selectfluor, THF; (e) bromoacetonitrile, K₂CO₃, CH₃CN, rt, 91.5%; (f) (i) aldehydes, piperidine (cat.), AcOH (cat.), toluene, reflux; (ii) 10% NaOH, CH₃OH, rt, 32-34%.

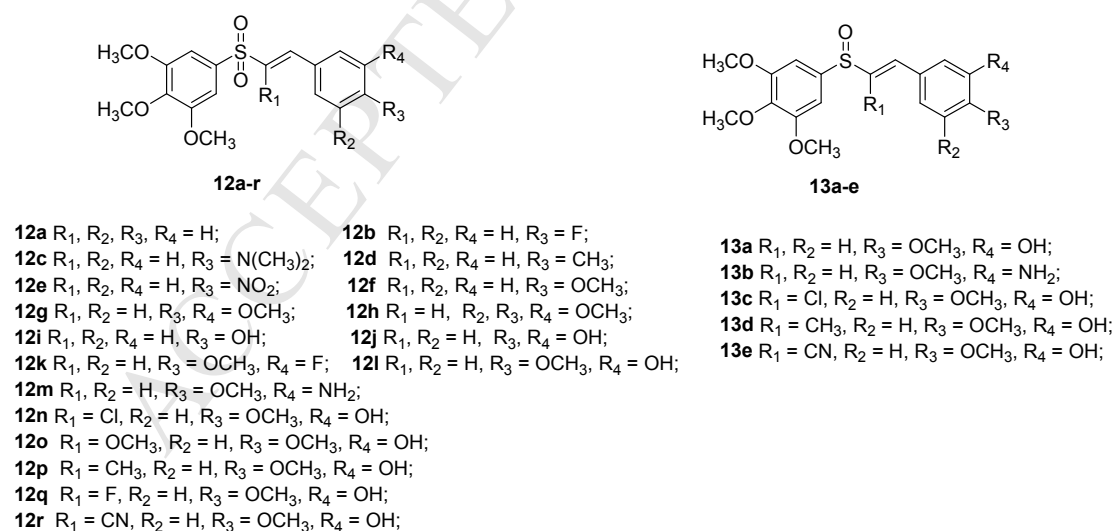


Fig. 3. The structures of vinyl sulfones **12a-r** and vinyl sulfoxides **13a-e**.

2.2 *In vitro* anti-proliferative activity

Given that ring B of classical CBSIs plays a vital effect on determining their binding affinities to tubulin, we firstly investigated the impact of this moiety on

activity. Thus, twelve compounds **12a-l** with varying substitutions on ring B were preliminarily screened for their anti-proliferative activities in human leukemia cell lines (K562) by the MTT assay. The results (see Supporting Information Fig. S1) indicated that compounds **12j** and **12l** displayed comparable anti-proliferative activities to the positive control CA-4 at a concentration of 1 μM . However, compound **12j** was inactive at the concentration of 0.1 μM , and the inhibitive rate of **12l** also decreased to 35.3%. Thus, compound **12l** bearing isovanillin as ring B was chosen for next round modifications.

Subsequently, eleven compounds **12m-r** and **13a-e** were further synthesized, and their anti-proliferative activities against three human cancer cell lines including human leukemia cell lines (K562), human hepatocellular carcinoma cells (HepG2) and human lung adenocarcinoma cells (A549), were evaluated by the MTT assay using compound **3** and CA-4 as the positive control. The cytotoxicity data of compounds **12l-r** and **13a-e** were listed in Table 1, and the results showed that most of the newly synthesized compounds displayed potent activities against three cancer cell lines. Vinyl sulfone **12l** and vinyl sulfoxide **13a**, whose R_1 were H exhibited more potent activity than the compounds with other substitutions as R_1 . Replacing R_1 with methyl group was not favorable for activity improvement, which is much different from the result that chalcone compound **4** was 20 folds increase in cytotoxicity towards **3** [10]. When R_1 was replaced with cyan group, both **12r** and **13e** showed much less potent activity. Interestingly, replacing hydroxyl with amino group (**12m**) led to slight improvements in anti-proliferative activities against K562, HepG2 and A549 cell lines with the IC_{50} values of 0.131, 0.217 and 0.606 μM , respectively.

2.3 *In vitro* tubulin polymerization inhibitory assay

To elucidate whether the synthesized compounds target the tubulin-microtubule system, the *in vitro* tubulin polymerization inhibition activities of **12l**, **12m**, **13a** and **13c** were evaluated due to their good anti-proliferative activities. The IC_{50} values listed in Table 2 showed that these compounds are potent tubulin polymerization inhibitors. Compound **13c** ($\text{IC}_{50} = 3.83 \mu\text{M}$) was the most potent compound in inhibiting tubulin polymerization which was comparable to compound **3** ($\text{IC}_{50} = 3.69 \mu\text{M}$) and slightly less potent than CA-4 ($\text{IC}_{50} = 2.17 \mu\text{M}$). Compound **12m** that displayed most potent anti-proliferative activity in the cytotoxic assay also showed potent activity in tubulin polymerization inhibition with an IC_{50} value of 4.25 μM . Therefore, taking considerations of the potent activities of compound **12m** showing both in the *in vitro* anti-proliferative assay and tubulin polymerization inhibition assay, **12m** was selected for further biological studies.

Table 1Anti-proliferative activities of compounds against three human cancer cell lines^a

Compd.	IC ₅₀ values (μ M) ^b		
	K562	HepG2	A549
12l	0.219 \pm 0.019	0.267 \pm 0.010	2.282 \pm 0.170
12m	0.128\pm0.003	0.217\pm0.015	0.606\pm0.084
12n	>1	>1	>5
12o	0.190 \pm 0.011	0.599 \pm 0.055	2.885 \pm 0.044
12p	0.580 \pm 0.031	0.710 \pm 0.102	2.734 \pm 0.153
12q	0.473 \pm 0.010	0.591 \pm 0.006	1.312 \pm 0.147
12r	>1	>1	>5
13a	0.258 \pm 0.008	0.307 \pm 0.038	1.455 \pm 0.291
13b	0.746 \pm 0.038	0.753 \pm 0.022	2.354 \pm 0.158
13c	0.183 \pm 0.009	0.243 \pm 0.042	1.204 \pm 0.254
13d	>1	>1	>5
13e	>1	>1	>5
3	0.060 \pm 0.009	0.102 \pm 0.013	0.387 \pm 0.026
CA-4	0.021 \pm 0.001	0.012 \pm 0.001	0.037 \pm 0.001

^a Cells were treated with different concentrations of the compounds for 72 h. Cell viability was measured by the MTT assay as described in the Experimental Section.

^b IC₅₀ values are indicated as the mean \pm SD (standard error) of at least three independent experiments.

Table 2

Effects of the selected compounds on tubulin polymerization inhibition.

Compd.	12l	12m	13a	13c	3	CA-4
IC ₅₀ values (μ M) ^a	8.23 \pm 0.92	4.25 \pm 0.75	7.18 \pm 0.88	3.83 \pm 0.42	3.69 \pm 0.13	2.17 \pm 0.02

^a IC₅₀ values are indicated as the mean \pm SD (standard error) of three independent experiments.

2.4 Anti-microtubule effects in K562 cells

Immunofluorescent assay was performed to investigate the effect of compound **12m** on microtubule networks. As shown in Fig. 4, K562 cells without drug treatment exhibited normal filamentous microtubules arrays. However, after exposure to **12m** (0.05 μ M, 0.10 μ M, 0.20 μ M) or CA-4 (0.005 μ M, 0.010 μ M, 0.020 μ M) for 24 h, the microtubule networks in cytosol were disrupted; these results indicated that **12m** can induce a dose-dependent collapse of the microtubule networks.

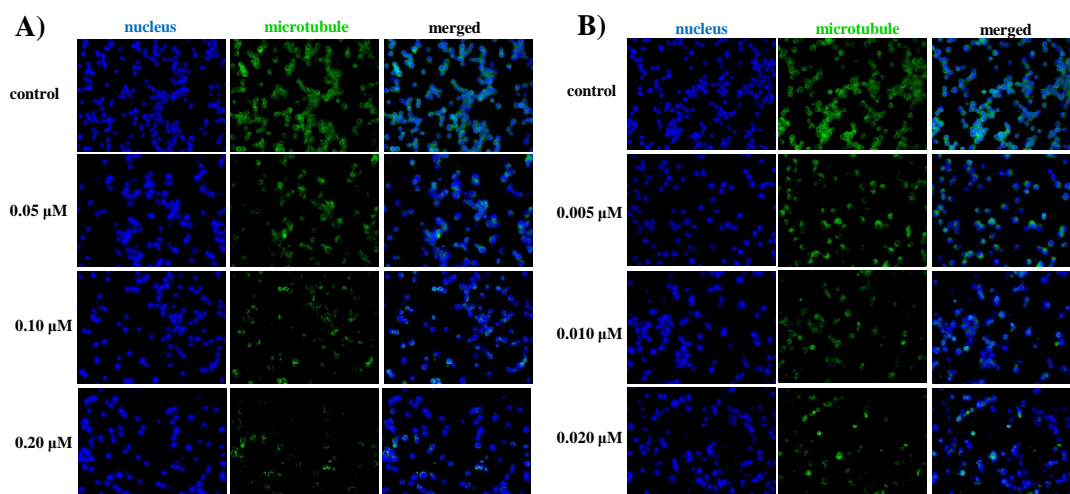


Fig. 4. Effects of compound **12m** (A) and CA-4 (B) on the cellular microtubule networks visualized by immunofluorescence. K562 cells were treated with vehicle control 0.1% DMSO, **12m** (0.05 μM , 0.10 μM , 0.20 μM), CA-4 (0.005 μM , 0.010 μM , 0.020 μM). Then, the cells were fixed and stained with anti- α -tubulin-FITC antibody (green), Alexa Fluor 488 dye and counterstained with DAPI (blue).

2.5 Cell cycle analysis

Most microtubule polymerization inhibitors disrupt cell mitosis and exert cell cycle arrest effects [21]. Thus, the effect of **12m** on cell cycle progression was examined using propidium iodide (PI) staining by flow cytometry analysis in K562 cells. As depicted in Fig. 5, compound **12m** caused a concentration-dependent G2/M arrest in K562 cells. When treated with **12m** at 0.05, 0.10, and 0.20 μM for 48 h, the percentages of cells arrested at the G2/M phase were 13.05%, 16.15%, and 21.99%, respectively, while that in the CA-4 treated groups were 13.84%, 22.59% and 24.95% at 0.005, 0.010, and 0.020 μM , respectively. These results demonstrated that compound **12m** can induce the cell cycle arrest at the G2/M phase.

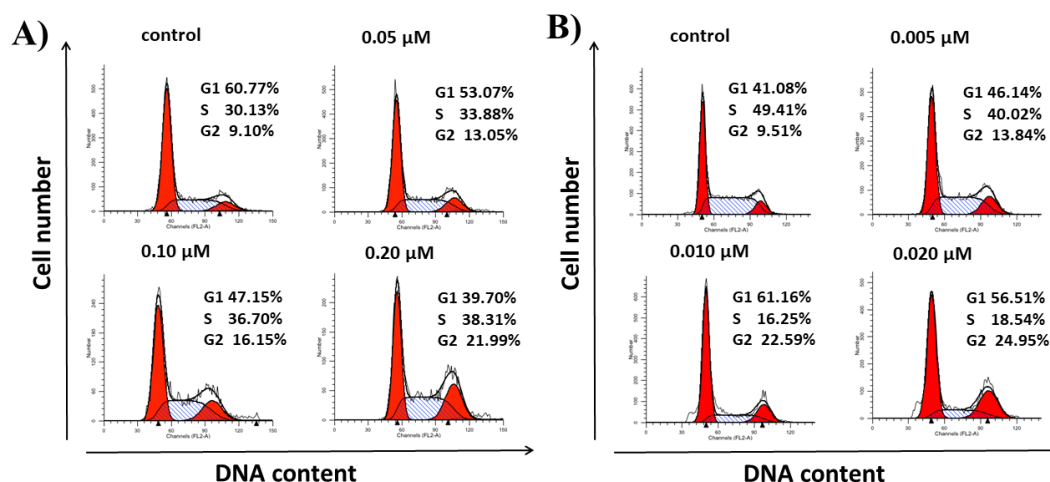


Fig. 5. Compound **12m** (A) and CA-4 (B) induced G2/M arrest in K562 cells. K562 cells were incubated with

varying concentrations of **12m** (0, 0.05, 0.1, and 0.2 μM) or CA-4 (0, 0.005, 0.010, and 0.020 μM) for 48 h. Cells were harvested and stained with PI and then analyzed by flow cytometry. The percentages of cells in different phases of cell cycle were analyzed by ModFit 4.1.

2.6 Cell apoptosis analysis

Most microtubule polymerization inhibitors can up-regulate the expression of pro-apoptotic proteins and down-regulate the expression of antiapoptotic proteins, thus inducing cell apoptosis [22]. To assess whether compound **12m** would induce cell apoptosis, **12m** treated K562 cells were stained with annexin V-FITC and propidium iodide (PI) and analyzed by flow cytometry. As shown in Fig. 6, compound **12m** induced K562 cell apoptosis in a dose-dependent manner. The percentage of apoptotic cells after the 48 h treatment was only 1.46% in the control group. However, the total numbers of early (Annexin $-V^+/PI^-$) and late (Annexin- V^+/PI^+) apoptotic cells increased to 17.88%, 22.65% and 49.29% after treatment with **12m** at 0.05, 0.10, 0.20 μM for 48 h, respectively (Fig. 6A). Similarly, after treatment with CA-4 at 0.005, 0.010, 0.020 μM for 48 h, the total numbers of early and late apoptotic cells increased to 25.28%, 53.05% and 63.05%, respectively (Fig. 6B). These results confirmed that compound **12m** and CA-4 effectively induced cell apoptosis in K562 cells in a dose-dependent manner (Fig. 6C and Fig. 6D).

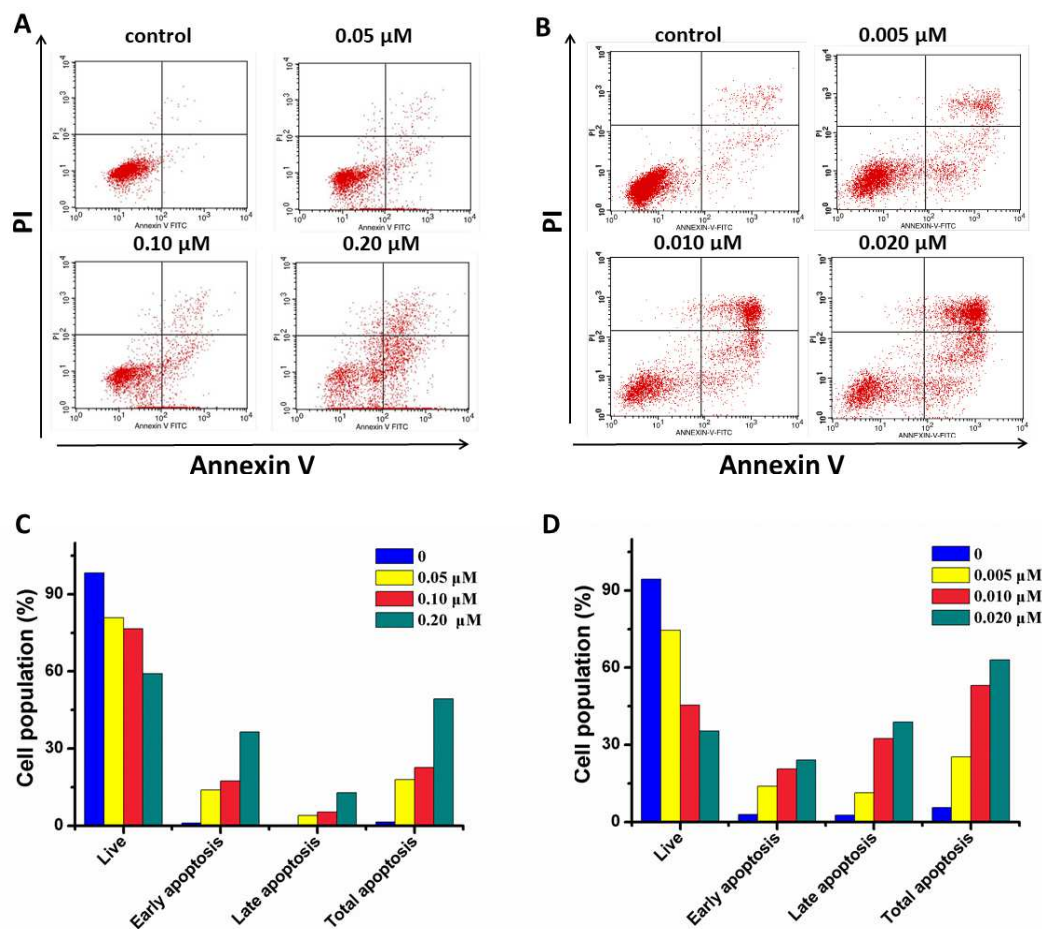


Fig. 6. (A) Compound **12m** induced apoptosis in K562 cells. K562 cells were incubated with varying concentrations of **12m** (0, 0.05, 0.1, and 0.2 μM). After 48 h of incubation, cells were collected and stained with Annexin-V/PI, followed by flow cytometric analysis. The percentages of cells in each stage of cell apoptosis were quantified by flow cytometry: (upper left quadrant) necrosis cells; (upper right quadrant) late-apoptotic cells; (bottom left quadrant) live cells; and (bottom right quadrant) early apoptotic cells. (B) CA-4 induced apoptosis in K562 cells. (C) Histograms display the percentage of cell distribution after treatment with **12m**. (D) Histograms display the percentage of cell distribution after treatment with CA-4.

2.7 *In vitro* evaluation of anti-vascular activity

Most CBSIs possess vascular disrupting activity, which is thought to disrupt microtubule dynamics to induce endothelial cell shape change. To evaluate the anti-vascular activity of compound **12m**, we used HUVEC culture assay to assess the ability of **12m** to inhibit HUVEC migration which is the key step to generate new blood vessels. As shown in Fig. 7A, the untreated cells migrated to fill the area that was initially scraped after 24 h. In contrast, compound **12m** and CA-4 significantly inhibited the HUVEC migration in a dose-dependent manner.

Then we evaluated the ability of compound **12m** in a tube formation assay. After being seeded on Matrigel, HUVECs form the capillary-like tubules with multicentric

junctions. After exposure to **12m** (0.05 μM , 0.10 μM , 0.20 μM) or CA-4 (0.005 μM , 0.010 μM , 0.020 μM) for 6 h, the capillary-like tubes were interrupted in different levels (Fig. 7B). These results showed that compound **12m** can effectively inhibit the tube formation of HUVECs.

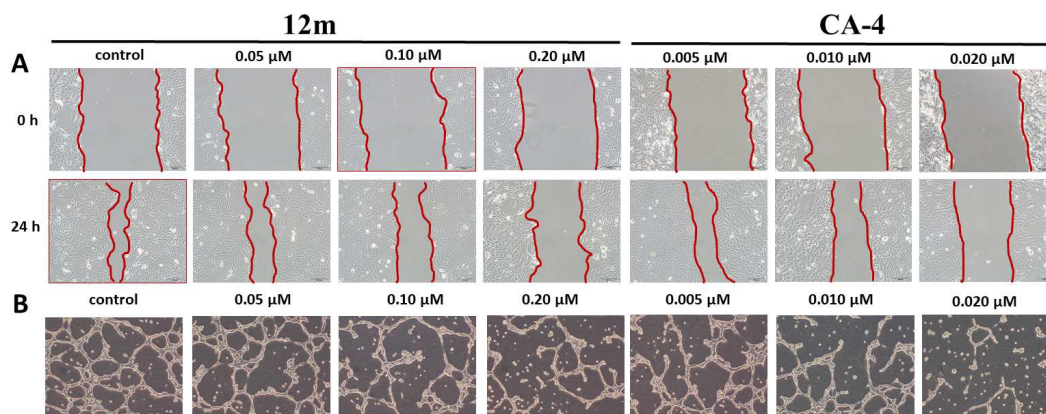


Fig. 7. Effects on the HUVECs migration and tube formation. (A) Scratches were created with sterile 200 μL pipette and images were captured using phase contrast microscopy at 0 h and 24 h after treatment with **12m** (0.05 μM , 0.10 μM , 0.20 μM) or CA-4 (0.005 μM , 0.010 μM , 0.020 μM). (B) Images depicting the formation of HUVEC capillary-like tubular network by treatment with **12m** (0.05 μM , 0.10 μM , 0.20 μM) or CA-4 (0.005 μM , 0.010 μM , 0.020 μM) for 6h.

2.8 *In vivo* anti-tumor activity of **12m**

To evaluate the *in vivo* anti-tumor activity of **12m**, liver cancer allograft mouse model was established by subcutaneous inoculation of H22 cells into the right flank of mice. The tumor size and the body weights of mice were monitored and recorded every 2 days. Paclitaxel (PTX) was selected as the positive control. As shown in Fig. 8, the reduction in tumor weight reached 74.60% at a dose of 8 mg/kg/2 day (i.v.) of PTX at 21 days after initiation of treatment as compared to vehicle. Treatment with **12m** at doses of 15 and 30 mg/kg/day (i.v.) resulted in tumor inhibitory rates of 53.4% and 65.4%, respectively, which is more potent than CA-4 treatment groups (inhibitory rates of 45.0% and 56.7% at doses of 15 and 30 mg/kg/day, respectively) (Fig. 8b). Notably, **12m** did not significantly affected body weight even at the dose up to 30 mg/kg, while treatment with PTX at a dose of 8 mg/kg/2 day led to a significant decrease of body weight (Fig. 8a). Thus, compound **12m** was efficacious and safe in inhibiting tumor growth with a dose-dependent manner *in vivo* and deserved further evaluation.

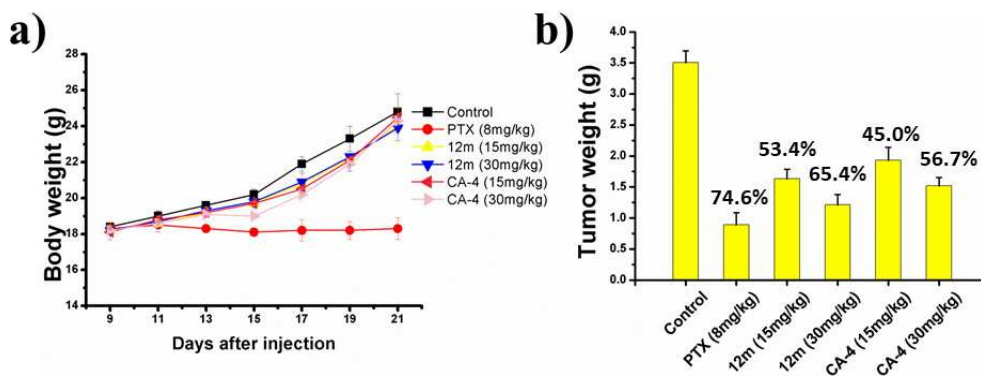


Fig. 8. a) Body weight changes of mice during treatment. (b) **12m** treatment resulted in significantly lower tumor weight compared with controls.

2.9 Docking study

To illustrate the binding mode of the most active compound **12m** with tubulin, docking study was performed by using the DOCK program in the Discovery Studio 3.0 software with the tubulin crystal structure (PDB: 1SA0). Resembling the binding mode of colchicine with tubulin (Fig. 9A), the trimethoxyphenyl moiety of **12m** was positioned in the binding cavity buried in tubulin while the Met259 and Thr314 residues hold the tail of **12m** (3-amino-4-methoyl phenyl moiety) (Fig. 9C). The introduction of methyl group on α position of carbonyl in chalcone compound **3** led to a dramatically improved cytotoxicity of compound **4**, which partly due to the more preferential *s-trans* conformation adopted by **4** [10]. Besides, the methyl located at α -position of carbonyl in compound **4** increased the hydrophobic interaction with the residue Lys254 (Fig. 9B). However, methyl group substituted at α -position of sulfone in compound **12p** didn't led to a significant improvement of activity, we speculated that the trimethoxyphenyl moiety of **12p** cannot be oriented into the deep cavity due to the hydrophobic interaction of methyl group with the residue Lys254 (Fig. 9C).

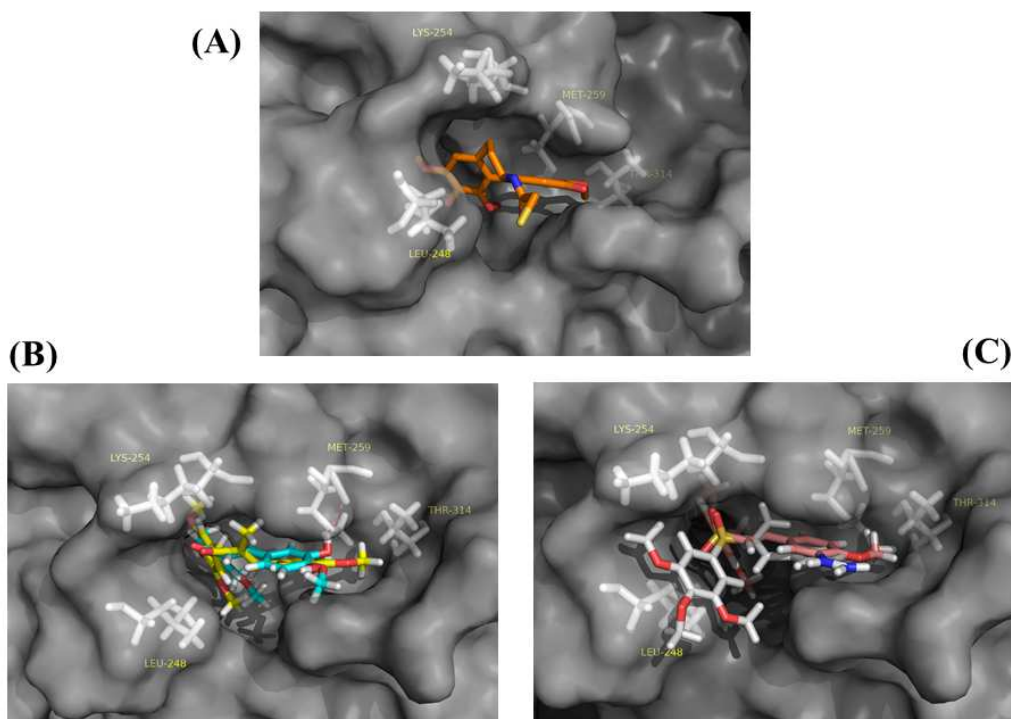


Fig. 9. Proposed binding models for representative compounds binding with tubulin (PDB code: 1SA0) (A) colchicine (shown in orange); (B) compound **3** (shown in cyan) and **4** (shown in yellow); (C) **12m** (shown in pink) and **12p** (shown in white).

3. Conclusions

In summary, a series of novel vinyl sulfone and sulfoxide derivatives have been designed, synthesized, and evaluated as tubulin polymerization inhibitors by replacing the carbonyl group of chalcone compound **3**. Preliminary anti-proliferative screening of twelve new compounds validated **12i** as a high cytotoxic compound. Following optimization of this lead resulted in the further synthesis and biological evaluations of eleven derivatives. Among them, compound **12m** showed the most potent activity against three cancer cell lines with IC_{50} values ranging from 0.128 to 0.606 μM . It was found that substitutions at α position of vinyl sulfones or sulfoxides were not favorable for the improvement of activity, which is unlike chalcone compound **3**. Besides, compound **12m** also displayed moderate inhibitory activity in tubulin assembly ($IC_{50} = 4.25 \mu\text{M}$). Furthermore, mechanism studies demonstrated that **12m** caused cell cycle arrest in the G2/M phase and induced cell apoptosis in K562 cells. And the immunofluorescent assay indicated that **12m** can effectively disrupt microtubule networks in a dose-dependent manner. The wound healing and tube formation assays further identified **12m** as a novel tubulin polymerization inhibitor with potent vascular disrupting activity. Moreover, molecular modelling studies demonstrated that **12m** interacted with tubulin at the colchicine binding site. Finally,

the *in vivo* anti-tumor activity of **12m** was validated in H22 liver cancer allograft mouse model with the tumor growth inhibitory activity more potent than CA-4. Altogether, vinyl sulfone derivative **12m** may represent a novel class of anti-tubulin agent with potent anti-vascular and anti-tumor activity and deserves further investigation.

4. Experimental

4.1 Chemistry

4.1.1. General

Most chemicals and solvents were purchased from commercial sources. Further purification and drying by standard methods were employed when necessary. ¹H NMR and ¹³C NMR spectra were recorded on Bruker-300 spectrometers in the indicated solvents (TMS as internal standard). Data are reported as follows: chemical shift in ppm (d), multiplicity (s =singlet, d =doublet, t =triplet, q =quartet, brs = broad singlet, m =multiplet), coupling constant (Hz), and integration. High Resolution Mass measurement was performed on Agilent QTOF 6520 mass spectrometer with electron spray ionization (ESI) as the ion source. Purity of all tested compounds was ≥ 95%, as estimated by HPLC analysis. Flash column chromatography was carried out using commercially available silica gel (200-300 mesh) under pressure.

4.1.2. Synthesis of intermediates **9a-d**

4.1.2.1. *3,4,5-Trimethoxybenzenethiol* **7**. 3,4,5-Trimethoxybenzenethiol **7** was synthesized according to literature report [21]. 3,4,5-trimethoxyaniline **5** (2.0 g, 10.9 mmol) was dissolved into the mixture of methanol (5 mL) and concentrated HCl (5 mL), sodium nitrite (1g, 14.4 mmol) dissolved with H₂O (5 mL) was added slowly at 0 °C. The temperature was kept below 5 °C and the reaction mixture was stirred until it became a clear solution, after which the reaction solution was added slowly to a solution of potassium ethyl xanthate (3.4 g, 21.2 mmol) in H₂O (20 mL) at 65 °C. The mixture was stirred at 65 °C for 30 min and cooled to room temperature. The resulting mixture was extracted with EtOAc (3 × 50 mL), and the combined organic extracts were then washed with brine (100 mL), dried over Na₂SO₄ and concentrated in vacuo. The crude product was purified by flash column chromatography (silica gel, PE/EA 15:1) affording xanthate **6** in 55.8% yield (1.73 g). Then, to a solution of xanthate **6** (1 g, 3.5 mmol) in ethanol (20 mL), a solution of sodium hydroxide (3 M, 20 mL) was added and the reaction was heated to 65 °C. The reaction was stirred at 65 °C for 3 h and cooled to room temperature. The mixture was acidified to pH 5 by the addition of 10% aqueous HCl and extracted with EtOAc (3 × 100 mL). The combined organic layers were then washed with brine (200 mL), dried over Na₂SO₄ and concentrated in

vacuo. The crude 3,4,5-trimethoxybenzenethiol **7** (640 mg, 94%) was used directly for the next step without further purification.

4.1.2.2. Intermediate 9a. To a solution of **7** (5.6 g, 28 mmol) in MeCN (50 mL), potassium carbonate (4.6 g, 33.6 mmol) was added. After stirring for 10 min, diethoxyphosphorylmethyl 4-methylbenzenesulfonate **8** was added into the mixture, and the reaction was stirred at 50 °C for 2 h. The reaction mixture was then extracted with EtOAc (3 × 100 mL). The combined organic layers were then washed with brine (100 mL), dried over anhydrous Na₂SO₄, and concentrated in vacuo. The residue was purified by flash column chromatography using CH₂Cl₂/MeOH (200/1, V/V) as an eluent to afford the product **9a** as yellow oil (600 mg, 63%). ¹H NMR (300 MHz, CDCl₃) δ 6.77 (s, 2H), 4.21-4.11 (m, 4H), 3.86 (s, 6H), 3.83 (s, 3H), 3.19 (d, *J* = 13.8 Hz, 2H), 1.33 (t, *J* = 7.0 Hz, 6H); ¹³C NMR (75 MHz, CDCl₃) δ 152.85, 137.04, 129.75 (d, *J* = 5.3 Hz), 107.44, 62.25 (d, *J* = 6.8 Hz), 60.38, 55.73, 29.20 (d, *J* = 147.8 Hz), 15.91 (d, *J* = 6.0 Hz); ESI-MS *m/z* 350.1 [M+Na]⁺ 373.1.

4.1.2.3. Intermediate 9b. To a solution of **9a** (1.9 g, 5.43 mmol) in CCl₄ (25 mL), NCS (863 mg, 6.52 mmol) was added. The mixture was stirred at room temperature for 2 hours. The insoluble materials were filtered off and the filtrate was concentrated in vacuo. The residue was purified by flash column chromatography using CH₂Cl₂/MeOH (200/1, V/V) as an eluent to afford the product **9b** as colorless oil (1.52 g, 72%). ¹H NMR (300 MHz, CDCl₃) δ 6.85 (s, 2H), 5.23 (d, *J* = 12.3 Hz, 1H), 4.30 (p, *J* = 7.1 Hz, 4H), 3.86 (s, 6H), 3.84 (s, 3H), 1.39 (t, *J* = 7.1 Hz, 6H); ¹³C NMR (75 MHz, CDCl₃) δ 152.93, 138.65, 126.07 (d, *J* = 10.5 Hz), 110.06, 64.11 (t, *J* = 6.0 Hz), 61.15 (d, *J* = 147.8 Hz), 60.37, 55.78, 15.93 (d, *J* = 6.0 Hz); ESI-MS *m/z* 384.1 [M-Cl]⁺ 349.1, [M+Na]⁺ 407.0.

4.1.2.4. Intermediate 9c. A solution of **9b** (500 mg, 1.42 mmol) in MeOH was refluxed for 30 min. The reaction mixture was concentrated in vacuo to afford the intermediate **9c** as yellow oil (488 mg, 90%). ¹H NMR (300 MHz, CDCl₃) δ 6.83 (s, 2H), 4.93 (d, *J* = 10.5 Hz, 1H), 4.32-4.09 (m, 4H), 3.83 (s, 6H), 3.82 (s, 3H), 3.55 (s, 3H), 1.34 (td, *J* = 7.0, 2.9 Hz, 6H); ¹³C NMR (75 MHz, CDCl₃) δ 152.71, 137.78, 128.25 (d, *J* = 7.5 Hz), 109.75, 86.35 (d, *J* = 179.3 Hz), 63.08 (m), 60.34, 56.57 (d, *J* = 10.5 Hz), 55.71, 15.95 (d, *J* = 6.0 Hz); ESI-MS *m/z* 380.1 [M+Na]⁺ 403.1.

4.1.2.5. Intermediate 9d. To a solution of **9a** (1 g, 2.86 mmol) in anhydrous THF, a solution of *n*-BuLi in *n*-hexane (2.5 M, 1.5 mL, 3.4 mmol) was added dropwise at -78 °C under N₂ atmosphere. After stirring for 30 min, a solution of CH₃I (212 μL, 3.1 mmol) in anhydrous THF was added, then the reaction was warmed up to room temperature and monitored by TLC. After reaction finished, the mixture was extracted with CH₂Cl₂ (3 × 50 mL). The combined organic layers were then washed with brine (50 mL), dried over anhydrous Na₂SO₄, and concentrated in vacuo. The residue was purified by flash column chromatography using CH₂Cl₂/MeOH (200/1, V/V) as an

eluent to afford the product **9d** as yellow oil (500 mg, 48%). ¹H NMR (300 MHz, CDCl₃) δ 6.83 (s, 2H), 4.19 (td, *J* = 7.3, 5.0 Hz, 4H), 3.87 (s, 6H), 3.84 (s, 3H), 3.25 (dd, *J* = 16.1, 7.4 Hz, 3H), 1.53 (dd, *J* = 17.1, 7.4 Hz, 3H), 1.34 (t, *J* = 7.1 Hz, 6H); ¹³C NMR (75 MHz, CDCl₃) δ 152.64, 137.54, 127.88 (d, *J* = 6.1 Hz), 109.75, 62.30 (dd, *J* = 12.4, 7.0 Hz), 60.34, 55.71, 38.95 (d, *J* = 141.8 Hz), 16.01 (d, *J* = 2.3 Hz), 15.93 (d, *J* = 1.5 Hz); ESI-MS *m/z* 364.1 [M+Na]⁺ 387.1.

4.1.3. Synthesis of intermediates **10a-e**.

4.1.3.1. General procedures for synthesis of intermediates **10a-d**. To a solution of **9a-d** (1 mmol) in CH₂Cl₂, *m*-CPBA (75%, 2.2 mmol) was added. After reaction completed, the mixture was extracted with CH₂Cl₂ (3 × 50 mL). The combined organic layers were then washed with saturated NaHCO₃, brine, dried over anhydrous Na₂SO₄, and concentrated in vacuo. The residue was purified by flash column chromatography to afford the products **10a-d** in 55-90% yields.

4.1.3.1.1 Intermediate **10a**. Colorless oil, yield 86.7%. ¹H NMR (300 MHz, CDCl₃) δ 7.21 (s, 2H), 4.27-4.08 (m, 4H), 3.91 (s, 6H), 3.89 (s, 3H), 3.76 (d, *J* = 17.0 Hz, 2H), 1.30 (t, *J* = 7.0 Hz, 6H); ¹³C NMR (75 MHz, CDCl₃) δ 152.80, 142.12, 134.14, 104.96, 62.84 (d, *J* = 6.0 Hz), 60.44, 56.00, 53.5 (d, *J* = 136.5 Hz), 15.75 (d, *J* = 6.0 Hz); ESI-MS *m/z* 382.1 [M+Na]⁺ 405.1.

4.1.3.1.2 Intermediate **10b**. Colorless oil, yield 55.4%. ¹H NMR (300 MHz, CDCl₃) δ 7.23 (s, 2H), 4.92 (d, *J* = 12.9 Hz, 1H), 4.36-4.23 (m, 4H), 3.92 (s, 4H), 3.92 (s, 6H), 1.36 (td, *J* = 7.0, 3.2 Hz, 6H); ¹³C NMR (75 MHz, CDCl₃) δ 152.58, 142.91, 129.73, 106.98, 65.88 (d, *J* = 155.3 Hz), 64.72 (m), 60.52, 56.03, 15.80 (d, *J* = 6.0 Hz); ESI-MS *m/z* 416.0 [M+Na]⁺ 439.0.

4.1.3.1.3 Intermediate **10c**. Colorless oil, yield 78.4%. ¹H NMR (300 MHz, CDCl₃) δ 7.18 (s, 2H), 4.48 (d, *J* = 12.4 Hz, 1H), 4.16-4.14 (m, 4H), 3.86 (s, 6H), 3.85 (s, 3H), 3.57 (s, 3H), 1.25 (m, 6H); ¹³C NMR (75 MHz, CDCl₃) δ 152.53, 142.42, 130.90, 106.60, 93.38 (d, *J* = 165.8 Hz), 63.63 (dd, *J* = 6.7, 3.5 Hz), 62.83 (d, *J* = 6.6 Hz), 60.41, 55.95, 15.78 (dd, *J* = 5.9, 3.1 Hz); ESI-MS *m/z* 412.1 [M+Na]⁺ 435.1.

4.1.3.1.4 Intermediate **10d**. Colorless oil, yield 90.3%. ¹H NMR (300 MHz, CDCl₃) δ 7.21 (s, 2H), 4.26-4.15 (m, 4H), 3.93 (s, 6H), 3.92 (s, 3H), 3.62 (dd, *J* = 19.0, 7.4 Hz, 1H), 1.56 (dd, *J* = 15.8, 7.4 Hz, 3H), 1.33 (t, *J* = 7.0 Hz, 6H); ¹³C NMR (75 MHz, CDCl₃) δ 152.62, 142.06, 132.12, 105.99, 62.84 (d, *J* = 6.0 Hz), 59.8 (d, *J* = 137.3 Hz), 55.98, 15.79 (dd, *J* = 6.2, 2.3 Hz), 11.01 (d, *J* = 4.1 Hz); ESI-MS *m/z* 396.1 [M+Na]⁺ 419.1.

4.1.3.2. Intermediate **10e**. To a solution of **10a** (500 mg, 1.31 mmol) in anhydrous THF, a solution of selectfluor (510 mg, 1.44 mmol) in DMF was added dropwise at 0°C. After reaction completed, the mixture was extracted with CH₂Cl₂ (3 × 50 mL).

The combined organic layers were then washed with saturated NaHCO₃, brine, dried over anhydrous Na₂SO₄, and concentrated in vacuo. The residue was purified by flash column chromatography using CH₂Cl₂/MeOH (150/1, V/V) as an eluent to afford the intermediate **10e** as yellow oil (270 mg, 51.6%). ¹H NMR (300 MHz, CDCl₃) δ 7.25 (s, 2H), 5.44 (dd, *J* = 45.6, 6.4 Hz, 1H), 4.41-4.28 (m, 4H), 3.97 (s, 3H), 3.96 (s, 6H), 1.41 (t, *J* = 7.1 Hz, 6H); ¹³C NMR (75 MHz, CDCl₃) δ 152.88, 143.01, 129.53, 106.30, 95.25 (d, *J* = 156.8 Hz), 64.50 (dd, *J* = 15.5, 6.7 Hz), 60.54, 56.05, 15.84 (d, *J* = 5.9 Hz); ESI-MS *m/z* 400.1 [M+Na]⁺ 423.1.

4.1.4. General procedures of intermediates **11a-d**.

To a solution of **9a-d** (1 mmol) in CH₂Cl₂, *m*-CPBA (75%, 0.95 mmol) were added slowly at 0 °C. After reaction completed, the mixture was extracted with CH₂Cl₂ (3 × 50 mL). The combined organic layers were then washed with brine, dried over anhydrous Na₂SO₄, and concentrated in vacuo. The residue was purified by flash column chromatography to afford the products **11a-d** in 58-82% yields.

4.1.4.1 Intermediate 11a. Colorless oil, yield 82.3%. ¹H NMR (300 MHz, CDCl₃) δ 6.93 (s, 2H), 4.22-4.02 (m, 4H), 3.87 (s, 6H), 3.82 (s, 3H), 3.30 (dt, *J* = 29.9, 14.6 Hz, 2H), 1.29 (dt, *J* = 14.8, 7.1 Hz, 6H); ¹³C NMR (75 MHz, CDCl₃) δ 153.49, 139.77, 138.92 (d, *J* = 8.4 Hz), 100.23, 62.36 (dd, *J* = 17.6, 6.4 Hz), 60.35, 55.87, 54.82 (d, *J* = 137.3 Hz), 15.79 (t, *J* = 5.7 Hz); ESI-MS *m/z* 366.1 [M+Na]⁺ 389.1.

4.1.4.2 Intermediate 11b. Colorless oil, yield 58.2%. Mixture of α and β isomers. ¹H NMR (300 MHz, CDCl₃) δ 7.08 (s, 0.7 H), 6.92 (s, 1.3H), 4.79 (d, *J* = 12.0 Hz, 0.35H), 4.55 (d, *J* = 12.0 Hz, 0.65H), 4.41-4.34 (m, 1.4H), 4.32-4.21 (m, 2.6H), 3.94 (s, 2.1H), 3.93 (s, 3.9H), 3.92 (s, 1H), 3.91 (s, 2.1H), 1.47-1.31 (m, 6H); ESI-MS *m/z* 400.1 [M+Na]⁺ 423.0.

4.1.4.3 Intermediate 11c. Colorless oil, yield 75.4%. Mixture of α and β isomers. ¹H NMR (300 MHz, CDCl₃) δ 7.06 (s, 1.5H), 7.01 (s, 0.4H), 4.44 (d, *J* = 7.5 Hz, 0.8H), 4.28-4.11 (m, 4H), 3.91 (s, 6H), 3.88 (s, 3H), 3.54 (s, 0.8H), 3.47 (s, 2.2H), 1.37-1.25 (m, 6H); ESI-MS *m/z* 396.1 [M+Na]⁺ 419.1.

4.1.4.4 Intermediate 11d. Colorless oil, yield 75.8%. Mixture of α and β isomers. ¹H NMR (300 MHz, CDCl₃) δ 7.02 (s, 1.4H), 6.84 (s, 0.6H), 4.29-4.14 (m, 2.8H), 4.14-4.08 (m, 1.2H), 3.91 (s, 4.2H), 3.91 (s, 2.1H), 3.89 (s, 1.8H), 3.88 (s, 0.9H), 3.38-3.29 (m, 0.7H), 2.97-2.86 (m, 0.3H), 1.39-1.19 (m, 9H); ESI-MS *m/z* 380.1 [M+Na]⁺ 403.1.

4.1.5. General procedures for synthesis of compounds 12a-k, 12m. To a solution of **10a** (0.2 mmol) in anhydrous THF, NaH (60%, 0.24 mmol) was added at 0 °C under N₂ atmosphere. After stirring for 15 min, aromatic aldehyde (0.24 mmol) was added into the mixture and the reaction was stirred for another 1 h. The reaction mixture was

then extracted with EtOAc (3 × 20 mL). The combined organic layers were then washed with saturated brine, dried over anhydrous Na₂SO₄, and concentrated in vacuo. The residue was purified by flash column chromatography using PE/EA (5/1,V/V) as an eluent to afford the compounds **12a-k**, **12m**.

4.1.5.1. (*E*)-1,2,3-trimethoxy-5-(styrylsulfonyl)benzene (**12a**). White solid, yield 76.7%, m.p. 122-124 °C. ¹H NMR (300 MHz, CDCl₃) δ 7.65 (d, *J* = 15.4 Hz, 1H), 7.45-7.17 (m, 5H), 7.17 (s, 2H), 6.87 (d, *J* = 15.4 Hz, 1H), 3.92 (s, 9H); ¹³C NMR (75 MHz, CDCl₃) δ 153.63, 141.86, 135.25, 132.44, 131.16, 129.09, 128.55, 127.47, 105.04, 60.93, 56.51; HR-MS (ESI) *m/z*: calcd for C₁₇H₁₈O₅S [M+H]⁺ 335.0948, found 335.0945.

4.1.5.2. (*E*)-5-((4-fluorostyryl)sulfonyl)-1,2,3-trimethoxybenzene (**12b**). White solid, yield 65.2%, m.p. 130-132 °C. ¹H NMR (300 MHz, CDCl₃) δ 7.61 (d, *J* = 15.4 Hz, 1H), 7.16 (s, 2H), 7.12-7.06 (m, 2H), 6.83-6.77 (d, *J* = 15.4 Hz, 1H), 5.32-4.90 (m, 1H), 3.91 (s, *J* = 5.3 Hz, 9H); ¹³C NMR (75 MHz, CDCl₃) δ 165.42 (d, *J* = 33.8 Hz), 153.15, 141.92, 140.02, 134.62, 130.08 (d, *J* = 6.8 Hz), 128.16, 126.72 (d, *J* = 2.3 Hz), 115.83 (d, *J* = 22.5 Hz), 104.51, 60.44, 56.01; HR-MS (ESI) *m/z*: calcd for C₁₇H₁₇FO₅S [M+H]⁺ 353.0853, found 353.0855.

4.1.5.3. (*E*)-*N,N*-dimethyl-4-(2-((3,4,5-trimethoxyphenyl)sulfonyl)vinyl)aniline (**12c**). Yellow solid, yield 65.3%, m.p. 175-177 °C. ¹H NMR (300 MHz, CDCl₃) δ 7.56 (d, *J* = 15.2 Hz, 1H), 7.37 (d, *J* = 8.8 Hz, 2H), 7.15 (s, 2H), 6.64 (d, *J* = 8.8 Hz, 2H), 6.58 (d, *J* = 15.2 Hz, 1H), 3.91 (s, 6H), 3.88 (s, 3H), 3.01 (s, 6H); ¹³C NMR (75 MHz, CDCl₃) δ 153.49, 152.28, 142.75, 141.85, 136.59, 130.37, 120.81, 119.25, 111.73, 104.68, 60.91, 56.47, 40.03; HR-MS (ESI) *m/z*: calcd for C₁₉H₂₃NO₅S [M+H]⁺ 378.1370, found 378.1366.

4.1.5.4. (*E*)-1,2,3-trimethoxy-5-((4-methylstyryl)sulfonyl)benzene (**12d**). White solid, yield 85.3%, m.p. 120-121 °C. ¹H NMR (300 MHz, CDCl₃) δ 7.62 (d, *J* = 15.4 Hz, 1H), 7.39 (d, *J* = 7.9 Hz, 2H), 7.20 (d, *J* = 8.1 Hz, 2H), 7.16 (s, 2H), 6.81 (d, *J* = 15.4 Hz, 1H), 3.91 (s, 6H), 3.90 (s, 3H), 2.37 (s, 3H); ¹³C NMR (75 MHz, CDCl₃) δ 153.10, 141.76, 141.45, 141.33, 134.98, 129.31, 129.18, 128.07, 125.72, 104.45, 60.43, 56.00, 20.98; HR-MS (ESI) *m/z*: calcd for C₁₈H₂₀O₅S [M+H]⁺ 349.1104, found 349.1103.

4.1.5.5. (*E*)-1,2,3-trimethoxy-5-((4-nitrostyryl)sulfonyl)benzene (**12e**). Yellow solid, yield 67.3%, m.p. 178-180 °C. ¹H NMR (300 MHz, CDCl₃) δ 8.17 (d, *J* = 8.6 Hz, 2H), 7.63-7.58 (m, 3H), 7.09 (s, 2H), 6.95 (d, *J* = 15.5 Hz, 1H), 3.85 (s, 6H), 3.84 (s, 3H); ¹³C NMR (75 MHz, CDCl₃) δ 153.76, 148.99, 142.83, 138.58, 138.46, 134.11, 131.83, 129.22, 124.26, 105.25, 60.98, 56.55; HR-MS (ESI) *m/z*: calcd for C₁₇H₁₇NO₇S [M+NH₄]⁺ 397.1064, found 397.1067.

4.1.5.6. (*E*)-1,2,3-trimethoxy-5-((4-methoxystyryl)sulfonyl)benzene (**12f**). White solid, yield 95.7%, m.p. 138-140 °C. ¹H NMR (300 MHz, CDCl₃) δ 7.60 (d, *J* = 15.3 Hz, 1H), 7.44 (d, *J* = 8.5 Hz, 2H), 7.16 (s, 2H), 6.91 (d, *J* = 8.4 Hz, 2H), 6.72 (d, *J* = 15.3

Hz, 1H), 3.91 (s, 6H), 3.89 (s, 3H), 3.83 (s, 3H); ^{13}C NMR (75 MHz, CDCl_3) δ 162.09, 153.58, 142.24, 141.68, 135.74, 130.35, 125.03, 124.61, 114.54, 104.87, 60.92, 56.49, 55.43; HR-MS (ESI) m/z : calcd for $\text{C}_{18}\text{H}_{20}\text{O}_6\text{S}$ $[\text{M}+\text{H}]^+$ 365.1053, found 365.1053.

4.1.5.7. (*E*)-5-((3,4-dimethoxystyryl)sulfonyl)-1,2,3-trimethoxybenzene (**12g**). White solid, yield 82.4%, m.p. 145-147 °C. ^1H NMR (300 MHz, CDCl_3) δ 7.59 (d, $J = 15.3$ Hz, 1H), 7.17 (s, 2H), 7.10 (d, $J = 8.3$ Hz, 1H), 6.99 (s, 1H), 6.87 (d, $J = 8.3$ Hz, 1H), 6.73 (d, $J = 15.3$ Hz, 1H), 3.92 (s, 6H), 3.90 (s, 3H), 3.89 (s, 3H); ^{13}C NMR (75 MHz, CDCl_3) δ 153.09, 151.41, 148.90, 145.67, 141.45, 135.15, 124.76, 124.32, 122.91, 110.66, 109.63, 104.43, 60.43, 56.00, 55.52, 55.47; HR-MS (ESI) m/z : calcd for $\text{C}_{19}\text{H}_{22}\text{O}_7\text{S}$ $[\text{M}+\text{H}]^+$ 395.1159, found 395.1165.

4.1.5.8. (*E*)-1,2,3-trimethoxy-5-(2-((3,4,5-trimethoxyphenyl)sulfonyl)vinyl)benzene (**12h**). White solid, yield 90.9%, m.p. 151-152 °C. ^1H NMR (300 MHz, CDCl_3) δ 7.56 (d, $J = 15.3$ Hz, 1H), 7.17 (s, 2H), 6.79 (d, $J = 15.3$ Hz, 1H), 6.72 (s, 2H), 3.92 (s, 6H), 3.90 (s, 3H), 3.87 (s, 9H); ^{13}C NMR (75 MHz, CDCl_3) δ 153.12, 153.06, 141.86, 141.44, 140.47, 134.81, 127.22, 125.94, 105.45, 104.51, 60.46, 56.01, 55.75; HR-MS (ESI) m/z : calcd for $\text{C}_{20}\text{H}_{24}\text{O}_8\text{S}$ $[\text{M}+\text{H}]^+$ 425.1265, found 425.1269.

4.1.5.9. (*E*)-4-(2-((3,4,5-trimethoxyphenyl)sulfonyl)vinyl)phenol (**12i**). Green solid, yield 89.0%, m.p. 155-157 °C. ^1H NMR (300 MHz, $\text{DMSO}-d_6$) δ 10.12 (s, 1H), 7.55 (d, $J = 7.9$ Hz, 2H), 7.49 (d, $J = 15.6$ Hz, 1H), 7.31 (d, $J = 15.6$ Hz, 1H), 7.15 (s, 1H), 6.79 (d, $J = 7.6$ Hz, 2H), 3.85 (s, 6H), 3.72 (s, 3H); ^{13}C NMR (75 MHz, $\text{DMSO}-d_6$) δ 160.83, 153.66, 142.12, 141.80, 136.67, 131.45, 124.26, 123.90, 116.32, 104.85, 60.67, 56.81; HR-MS (ESI) m/z : calcd for $\text{C}_{20}\text{H}_{24}\text{O}_8\text{S}$ $[\text{M}+\text{H}]^+$ 351.0902, found 351.0905.

4.1.5.10. (*E*)-4-(2-((3,4,5-trimethoxyphenyl)sulfonyl)vinyl)benzene-1,2-diol (**12j**). Green solid, yield 88.5%, m.p. 186-188 °C. ^1H NMR (300 MHz, $\text{DMSO}-d_6$) δ 9.73 (s, 1H), 7.15 (s, 1H), 7.42 (d, $J = 15.3$ Hz, 1H), 7.26 (d, $J = 15.2$ Hz, 1H), 7.18 (s, 2H), 7.08 (s, 1H), 7.05 (d, $J = 9.0$ Hz, 1H), 6.79 (d, $J = 8.1$ Hz, 1H), 3.88 (s, 6H), 3.75 (s, 3H); ^{13}C NMR (75 MHz, $\text{DMSO}-d_6$) δ 153.14, 148.95, 145.62, 142.00, 141.29, 136.24, 123.96, 123.83, 122.05, 115.68, 115.48, 104.35, 60.16, 56.31; HR-MS (ESI) m/z : calcd for $\text{C}_{17}\text{H}_{18}\text{O}_7\text{S}$ $[\text{M}+\text{H}]^+$ 367.0846, found 367.0845.

4.1.5.11. (*E*)-5-((3-fluoro-4-methoxystyryl)sulfonyl)-1,2,3-trimethoxybenzene (**12k**). White solid, yield 95.9%, m.p. 170-172 °C. ^1H NMR (300 MHz, CDCl_3) δ 7.54 (d, $J = 15.2$ Hz, 1H), 7.25-7.22 (m, 2H), 7.16 (s, 2H), 6.96 (d, $J = 8.3$ Hz, 1H), 6.73 (d, $J = 15.3$ Hz, 1H), 3.92 (s, 12H); ^{13}C NMR (75 MHz, CDCl_3) δ 154.02, 153.62, 150.52 (d, $J = 12.9$ Hz), 140.51, 135.32, 126.21, 126.11 (d, $J = 3.0$ Hz), 125.51 (d, $J = 6.8$ Hz), 124.16 (d, $J = 39.8$ Hz), 115.15 (d, $J = 18.8$ Hz), 113.32, 104.96, 60.92, 56.50, 56.28; HR-MS (ESI) m/z : calcd for $\text{C}_{18}\text{H}_{19}\text{FO}_6\text{S}$ $[\text{M}+\text{H}]^+$ 383.0959, found 383.0963.

4.1.5.12. (*E*)-2-methoxy-5-(2-((3,4,5-trimethoxyphenyl)sulfonyl)vinyl)aniline (**12m**). Yellow solid, yield 60%, m.p. 104-106 °C. ^1H NMR (300 MHz, CDCl_3) δ 7.52 (d, $J =$

15.3 Hz, 1H), 7.14 (s, 2H), 6.89 (dd, $J = 8.2, 2.0$ Hz, 1H), 6.84 (d, $J = 2.0$ Hz, 1H), 6.76 (d, $J = 8.3$ Hz, 1H), 6.65 (d, $J = 15.3$ Hz, 1H), 3.87-3.91 (m, 12H); ^{13}C NMR (75 MHz, CDCl_3) δ 153.01, 149.43, 142.01, 141.41, 136.31, 135.38, 124.78, 123.52, 120.38, 112.64, 109.62, 104.15, 60.47, 55.96, 55.11; HR-MS (ESI) m/z : calcd for $\text{C}_{18}\text{H}_{21}\text{NO}_6\text{S}$ $[\text{M}+\text{H}]^+$ 380.1162, found 380.1167.

4.1.6 General procedures for synthesis of compounds **12l**, **12n-q**, **13a-d**.

To a solution of **10a-d** (0.2 mmol) in anhydrous THF, NaH (60%, 0.24 mmol) was added at 0 °C under N_2 atmosphere. After stirring for 15 min, acetyl protected isovanillin (0.24 mmol) was added into the mixture and the reaction was stirred for another 1 h. The reaction mixture was then extracted with EtOAc (3×20 mL). The combined organic layers were then washed with saturated brine, dried over anhydrous Na_2SO_4 , and concentrated in vacuo. The residue was dissolved in MeOH (5 mL), 5% sodium hydroxide (5 mL) was added. After stirring for 30 min at room temperature, the reaction mixture was acidified by the addition of 10% aqueous HCl, and then diluted with EtOAc, washed with water, and brine successively, dried over anhydrous Na_2SO_4 , and concentrated in vacuo. The residue was purified by flash column chromatography using PE/EA (4/1, V/V) as an eluent to afford the compounds **12l**, **12n-q**, **13a-d**.

4.1.6.1. (*E*)-2-methoxy-5-(2-((3,4,5-trimethoxyphenyl)sulfonyl)vinyl)phenol (**12l**). White solid, yield 87.0%, m.p. 127-129 °C. ^1H NMR (300 MHz, $\text{DMSO}-d_6$) δ 9.20 (s, 1H), 7.45 (d, $J = 15.3$ Hz, 1H), 7.33 (d, $J = 15.3$ Hz, 1H), 7.17 (s, 2H), 7.15-7.09 (m, 2H), 6.97 (d, $J = 8.3$ Hz, 1H), 3.86 (s, 6H), 3.81 (s, 3H), 3.73 (s, 3H); ^{13}C NMR (75 MHz, $\text{DMSO}-d_6$) δ 153.65, 151.02, 147.18, 142.12, 141.84, 136.52, 125.73, 125.62, 122.47, 115.33, 112.40, 104.92, 60.67, 56.82, 56.16; HR-MS (ESI) m/z : calcd for $\text{C}_{18}\text{H}_{20}\text{O}_7\text{S}$ $[\text{M}+\text{H}]^+$ 381.1003, found 381.1004.

4.1.6.2. (*Z*)-2-methoxy-5-(2-chloro-2-((3,4,5-trimethoxyphenyl)sulfonyl)vinyl)phenol (**12n**). Yellow oil, yield 44.2%. ^1H NMR (300 MHz, CDCl_3) δ 7.83 (s, 1H), 7.45 (d, $J = 1.8$ Hz, 1H), 7.25-7.22 (m, 2H), 7.11 (s, 2H), 6.81 (d, $J = 8.5$ Hz, 1H), 3.85 (s, 3H), 3.85 (s, 9H); ^{13}C NMR (75 MHz, CDCl_3) δ 152.87, 148.52, 145.11, 142.22, 133.90, 131.43, 128.28, 124.10, 124.06, 115.36, 109.97, 105.72, 60.51, 56.03, 55.52; HR-MS (ESI) m/z : calcd for $\text{C}_{18}\text{H}_{19}\text{ClO}_7\text{S}$ $[\text{M}+\text{H}]^+$ 415.0613, found 415.0623.

4.1.6.3. (*E*)-2-methoxy-5-(2-methoxy-2-((3,4,5-trimethoxyphenyl)sulfonyl)vinyl)phenol (**12o**). Yellow oil, yield 57.1%. ^1H NMR (300 MHz, CDCl_3) δ 7.32 (d, $J = 2.0$ Hz, 1H), 7.18 (s, 2H), 7.13 (dd, $J = 8.4$ Hz, 2.1 Hz, 1H), 7.11 (s, 1H), 6.86 (d, $J = 8.4$ Hz, 1H), 5.77 (s, 1H), 3.92 (s, 9H), 3.90 (s, 3H), 3.89 (s, 3H); ^{13}C NMR (75 MHz, CDCl_3) δ 152.89, 151.05, 147.53, 145.26, 141.83, 133.19, 124.22, 122.86, 122.03, 114.86, 110.06, 105.01, 61.34, 60.47, 55.97, 55.46; HR-MS (ESI) m/z : calcd for $\text{C}_{19}\text{H}_{22}\text{O}_8\text{S}$ $[\text{M}+\text{H}]^+$ 411.1108, found 411.1111.

4.1.6.4. (*E*)-2-methoxy-5-(2-((3,4,5-trimethoxyphenyl)sulfonyl)prop-1-en-1-yl)phenol (**12p**). White solid, yield 37.5%, m.p. 145-147 °C. ¹H NMR (300 MHz, DMSO-*d*₆) δ 9.21 (s, 1H), 7.53(s, 1H), 7.06 (s, 2H), 6.96 (s, 3H), 3.81 (s, 6H), 3.76 (s, 3H), 3.70 (s, 3H), 2.04 (s, 3H); ¹³C NMR (75 MHz, DMSO-*d*₆) δ 153.68, 149.56, 146.94, 142.00, 137.32, 134.57, 134.51, 126.59, 122.85, 117.11, 112.54, 105.63, 60.68, 56.87, 56.08, 13.64; HR-MS (ESI) m/z: calcd for C₁₉H₂₂O₇S [M+H]⁺ 395.1159, found 395.1158.

4.1.6.5. (*E*)-2-methoxy-5-(2-fluoro-2-((3,4,5-trimethoxyphenyl)sulfonyl)vinyl)phenol (**12q**). White solid, yield 27.6%, m.p. 120-122 °C. ¹H NMR (300 MHz, CDCl₃) δ 7.22 (d, *J* = 1.9 Hz, 1H), 7.20 (s, 2H), 7.10 (dd, *J* = 8.3, 1.8 Hz, 1H), 6.92 (d, *J* = 42 Hz, 1H), 6.87 (s, 1H), 5.66 (s, 1H), 3.93 (s, 6H), 3.92 (s, 6H); ¹³C NMR (75 MHz, CDCl₃) δ 153.08, 147.87, 145.24, 131.50, 123.12, 123.03, 122.41, 115.42, 115.31, 114.74, 110.09, 105.25, 60.54, 56.04, 55.97, 55.49; HR-MS (ESI) m/z: calcd for C₁₈H₁₉FO₇S [M+NH₄]⁺ 416.1174, found 416.1177.

4.1.6.6. (*E*)-2-methoxy-5-(2-((3,4,5-trimethoxyphenyl)sulfinyl)vinyl)phenol (**13a**). White solid, yield 28.6%, m.p. 130-132 °C. ¹H NMR (300 MHz, CDCl₃) δ 7.25 (d, *J* = 15.8 Hz, 1H), 7.06 (d, *J* = 1.8 Hz, 1H), 6.97 (dd, *J* = 8.3, 1.8 Hz, 1H), 6.90 (s, 2H), 6.83 (d, *J* = 8.3 Hz, 1H), 6.68 (d, *J* = 15.5 Hz, 1H), 6.04 (s, 1H), 3.90 (s, 9H), 3.87 (s, 3H); ¹³C NMR (75 MHz, CDCl₃) δ 153.59, 147.91, 145.50, 139.51, 138.35, 136.66, 130.20, 126.66, 120.78, 112.54, 110.13, 100.84, 60.42, 55.88, 55.51; HR-MS (ESI) m/z: calcd for C₁₈H₂₀O₆S [M+H]⁺ 365.1053, found 365.1054.

4.1.6.7. (*E*)-2-methoxy-5-(2-((3,4,5-trimethoxyphenyl)sulfinyl)vinyl)aniline (**13b**). White solid, yield 35.4%, m.p. 100-102 °C. ¹H NMR (300 MHz, CDCl₃) δ 7.23 (d, *J* = 15.6 Hz, 1H), 6.89 (s, 2H), 6.88-6.83 (m, 2H), 6.75 (d, *J* = 8.1 Hz, 1H), 6.64 (d, *J* = 15.5 Hz, 1H), 3.90 (s, 6H), 3.87 (s, 6H); ¹³C NMR (75 MHz, CDCl₃) δ 153.55, 148.53, 139.36, 138.70, 137.49, 136.09, 129.58, 126.17, 119.18, 112.40, 109.64, 100.78, 60.43, 55.88, 55.09; HR-MS (ESI) m/z: calcd for C₁₈H₂₁NO₅S [M+H]⁺ 364.1213, found 364.1212.

4.1.6.8. (*Z*)-2-methoxy-5-(2-chloro-2-((3,4,5-trimethoxyphenyl)sulfinyl)vinyl) phenol (**13c**). Yellow oil, yield 55.6%. ¹H NMR (300 MHz, CDCl₃) δ 7.24 (s, 1H), 7.15 (d, *J* = 2.0 Hz, 1H), 7.04 (dd, *J* = 2.1 Hz, 8.5Hz, 1H), 6.91 (d, *J* = 8.3 Hz, 1H), 6.82 (s, 2H), 5.96 (s, 1H), 3.94 (s, 3H), 3.88 (s, 3H), 3.86 (s, 6H); ¹³C NMR (75 MHz, CDCl₃) δ 153.36, 147.36, 145.37, 139.82, 137.85, 137.69, 135.50, 125.27, 121.87, 114.99, 110.20, 101.05, 60.47, 55.65, 55.53; HR-MS (ESI) m/z: calcd for C₁₈H₁₉ClO₆S [M+H]⁺ 390.0669, found 399.0660.

4.1.6.8. (*E*)-2-methoxy-5-(2-((3,4,5-trimethoxyphenyl)sulfinyl)prop-1-en-1-yl)phenol (**13d**). White solid, yield 40.6%, m.p. 135-137 °C. Mixture of α and β isomers (1:1), ¹H NMR (300 MHz, CDCl₃) δ 7.26 (s, 0.5H), 7.10 (d, *J* = 2.0 Hz, 0.5H), 7.04 (d, *J* = 2.0 Hz, 0.5H), 7.03 (dd, *J* = 8.4, 1.9 Hz, 0.5H), 6.95 (dd, *J* = 8.4, 1.9 Hz, 0.5H), 6.90 (s, 0.5H), 6.89 (s, 1H), 6.86 (s, 1H), 6.74 (s, 1H), 6.20 (s, 0.5H), 6.10 (s, 0.5H), 3.91

(s, 3H), 3.88 (s, 4.5H), 3.86 (s, 1.5H), 3.83 (s, 3H), 1.93 (d, $J = 1.2$ Hz, 1.5H), 1.91 (d, $J = 1.3$ Hz, 1.5H); HR-MS (ESI) m/z : calcd for $C_{19}H_{22}O_6S$ $[M+H]^+$ 379.1210, found 379.1210.

4.1.7. Synthesis of target compounds **12r** and **13e**.

4.1.7.1. *Intermediate 14*. To a solution of **7** (750 mg, 3.75 mmol) in MeCN, potassium carbonate (621 mg, 4.5 mmol) was added. After stirring for 10 min, bromoacetonitrile (313 μ L, 4.5 mmol) was added into the mixture, then the reaction was stirred at room temperature for 1 h. the mixture was extracted with CH_2Cl_2 (3×50 mL). The combined organic layers were then washed with brine, dried over anhydrous Na_2SO_4 , and concentrated in vacuo to afford the crude product **14** as gray solid (820 mg, 91.5%), which was used directly for the next step without further purification, m.p. 109-111 $^{\circ}C$. 1H NMR (300 MHz, $CDCl_3$) δ 6.83 (s, 2H), 3.88 (s, 6H), 3.85 (s, 3H), 3.57 (s, 2H); ^{13}C NMR (75 MHz, $CDCl_3$) δ 153.04, 138.55, 125.95, 116.48, 110.05, 55.82, 43.04, 21.80; ESI-MS m/z 239.1 $[M+Na]^+$ 262.0.

4.1.7.2. *Intermediate 15*. To a solution of **14** (600 mg, 2.51 mmol) in CH_2Cl_2 , *m*-CPBA (75%, 1.27 g, 5.52 mmol) was added. The reaction mixture was stirred for 1 h, and then was extracted with CH_2Cl_2 (3×50 mL). The combined organic layers were then washed with saturated $NaHCO_3$, brine, dried over anhydrous Na_2SO_4 , and concentrated in vacuo to afford the crude product **15** as gray solid (620 mg, 91.2%), which was used directly for the next step without further purification, m.p. 139-141 $^{\circ}C$. 1H NMR (300 MHz, $CDCl_3$) δ 7.26 (s, 2H), 4.15 (s, 2H), 3.99 (s, 3H), 3.98 (s, 6H); ^{13}C NMR (75 MHz, $CDCl_3$) δ 153.20, 143.25, 130.33, 110.27, 105.51, 60.61, 56.12, 45.39; ESI-MS m/z 271.1 $[M-H]^-$ 270.1.

4.1.7.3. *Intermediate 16*. To a solution of **14** (600 mg, 2.51 mmol) in CH_2Cl_2 , *m*-CPBA (75%, 262 mg, 2.13 mmol) was added slowly at 0 $^{\circ}C$. The reaction mixture was stirred for 1 h, and then was extracted with CH_2Cl_2 (3×50 mL). The combined organic layers were then washed with saturated $NaHCO_3$, brine, dried over anhydrous Na_2SO_4 , and concentrated in vacuo to afford the crude product **16** as gray solid (364 mg, 56.9%), which was used directly for the next step without further purification, m.p. 126-128 $^{\circ}C$. 1H NMR (300 MHz, $CDCl_3$) δ 6.98 (s, 2H), 3.94 (s, 6H), 3.91 (s, 3H), 3.76 (dd, $J = 38.6, 15.7$ Hz, 2H); ^{13}C NMR (75 MHz, $CDCl_3$) δ 153.76, 140.79, 135.32, 110.84, 100.37, 60.48, 55.99, 44.37; ESI-MS m/z 255.1 $[M+Na]^+$ 278.0.

4.1.7.4. (*E*)-2-((3,4,5-trimethoxyphenyl)sulfonyl)-3-(3-hydroxy-4-methoxyphenyl) acrylonitrile (**12r**). To a solution of **15** (80 mg, 0.3 mmol) and acetyl protected isovanillin (63 mg, 0.33 mmol) in toluene, piperidine (cat, 5 μ L) and AcOH (cat, 5 μ L) was added, and the mixture was refluxed and monitored by TLC. After reaction completed, toluene was removed in vacuo and the residue was extracted with EtOAc (3×50 mL). The combined organic layers were then washed with brine, dried over anhydrous Na_2SO_4 , and concentrated in vacuo to afford crude product **17** or **18**. Then,

the crude was dissolved in MeOH (5 mL), 5% sodium hydroxide (5 mL) was added. After stirring for 30 min at room temperature, the reaction mixture was acidified by the addition of 10% aqueous HCl, and then diluted with EtOAc, washed with water, and brine successively, dried over anhydrous Na₂SO₄, and concentrated in vacuo. The residue was purified by flash column chromatography using PE/EA (3/2,V/V) as an eluent to afford the compound **12r** as yellow solid (30 mg, 31.1%). ¹H NMR (300 MHz, CDCl₃) δ 7.95 (s, 1H), 7.48 (d, *J* = 2.1 Hz, 1H), 7.38 (dd, *J* = 8.5, 2.1 Hz, 1H), 7.12 (s, 2H), 6.85 (d, *J* = 8.5 Hz, 1H), 3.88 (s, 3H), 3.85 (s, 6H), 3.84 (s, 3H); ¹³C NMR (75 MHz, CDCl₃) δ 153.13, 151.54, 150.31, 145.83, 142.50, 132.16, 125.71, 123.07, 115.47, 113.28, 110.73, 110.41, 105.17, 60.53, 56.06, 55.74; HR-MS (ESI) *m/z*: calcd for C₁₉H₁₉NO₇S [M+NH₄]⁺ 423.1220, found 423.1223.

4.1.7.5. (*E*)-2-((3,4,5-trimethoxyphenyl)sulfinyl)-3-(3-hydroxy-4-methoxyphenyl)acrylonitrile (**13e**). Compound **13e** was prepared by the same method as compound **12r**. Yellow solid, yield 29.0%, m.p. 185-187 °C. ¹H NMR (300 MHz, CDCl₃) δ 7.69 (s, 1H), 7.51 (d, *J* = 2.0 Hz, 1H), 7.43 (dd, *J* = 8.5, 2.0 Hz, 1H), 6.96 (s, 2H), 6.91 (d, *J* = 8.5 Hz, 1H), 3.95 (s, 3H), 3.91 (s, 6H), 3.89 (s, 3H); ¹³C NMR (75 MHz, CDCl₃) δ 153.64, 149.94, 145.54, 144.05, 140.60, 135.70, 124.37, 123.90, 115.03, 114.23, 113.19, 110.25, 101.19, 60.48, 55.97, 55.65; HR-MS (ESI) *m/z*: calcd for C₁₉H₁₉NO₆S [M+H]⁺ 390.1011, found 390.1012.

4.2 Pharmacology

4.2.1 *In vitro* anti-proliferative assay

K562, HepG2 and A549 cells were purchased from Nanjing KeyGen Biotech Co. Ltd. (Nanjing, China). The cytotoxicity of the test compounds was determined using the MTT assay. Briefly, the cell lines were incubated at 37 °C in a humidified 5% CO₂ incubator for 24 h in 96-microwell plates. After medium removal, 100 μL of culture medium with 0.1% DMSO containing the test compounds at different concentrations was added to each well and incubated at 37 °C for another 72 h. The MTT (5 mg/mL in PBS) was added and incubated for another 4 h, the optical density was detected with a microplate reader at 490 nm. The IC₅₀ values were calculated according to the dose-dependent curves. All the experiments were repeated in at least three independent experiments.

4.2.2 *In vitro* tubulin polymerization inhibitory assay

An amount of 2 mg/mL tubulin (Cytoskeleton) was resuspended in PEM buffer containing 80 mM piperazine-N,N'-bis(2-ethanesulfonic acid) sequeisodium salt PIPES (pH 6.9), 0.5 mM EGTA, 2 mM MgCl₂, and 15% glycerol. Then the mixture was preincubated with compounds or vehicle DMSO on ice. PEG containing GTP was added to the final concentration of 3 mg/mL before detecting the tubulin

polymerization reaction. After 30 min, the absorbance of different concentrations was detected by a spectrophotometer at 340 nm at 37 °C. The area under the curve was used to determine the concentration that inhibited tubulin polymerization by 50% (IC₅₀), which was calculated with GraphPad Prism Software version 5.02.

4.2.3 Immunofluorescence Staining

K562 cells were seeded into 6-well plates and then treated with vehicle control 0.1% DMSO, **12m** (0.05 μ M, 0.1 μ M, 0.2 μ M). The cells were fixed with 4% paraformaldehyde and then penetrated with PBS for three times. After blocking for 20 min by adding 50-100 μ L goat serum albumin at room temperature, cells were incubated with a monoclonal antibody (anti- α -tubulin) at 37 °C for 2 h. Then the cells were washed three times by PBS following staining by fluorescence antibody and labeling of nuclei by 4,6-diamidino-2-phenylindole (DAPI). Cells were finally visualized using a fluorescence microscope (OLYMPUS, Japan).

4.2.4 Cell cycle analysis

K562 cells were seeded into 6-well plates and incubated at 37 °C in a humidified 5% CO₂ incubator for 24 h, and then treated with or without **12m** at indicated concentrations for another 72 h. The collected cells were fixed by adding 70% ethanol at 4 °C for 12 h. Subsequently, the cells were resuspended in PBS containing 100 mL RNase A and 400 mL of propidium iodide for 30 min. The DNA content of the cells was measured using a FACS Calibur flow cytometer (Bectone Dickinson, San Jose, CA, USA).

4.2.5 Cell apoptosis analysis

After treatment with or without **12m** at indicated concentrations for 72 h, the cells were washed twice in PBS, centrifuged and resuspended in 500 mL AnnexinV binding buffer. The cells were then harvested, washed and stained with 5 mL Annexin V-APC and 5 mL 7-AAD in the darkness for 15 min. Apoptosis was analyzed using a FACS Calibur flow cytometer (Bectone Dickinson, San Jose, CA, USA).

4.2.6 Wound healing assay

K562 cells were grown in 6-well plates for 24 h. Scratches were made in confluent monolayers using 200 μ L pipette tip. Then, wounds were washed twice with PBS to remove non-adherent cell debris. The media containing different concentrations (0, 0.05, 0.1, 0.2 μ M) of the compound **12m** were added to the petridishes. Cells which migrated across the wound area were photographed using phase contrast microscopy at 0 h and 24 h. The migration distance of cells migrated in to the wound area was measured manually.

4.2.7 Tube formation assay

EC Matrigel matrix was thawed at 4 °C overnight, and HUVECs suspended in DMEM were seeded in 96-well culture plates at a cell density of 50,000 cells/well after polymerization of the Matrigel at 37 °C for 30 min. They were then treated with 20 μ L different concentrations of compound **12m** or vehicle for 6 h at 37 °C. Then, the morphological changes of the cells and tubes formed were observed and photographed under inverted microscope (OLYMPUS, Japan).

4.2.8 In vivo anti-tumor evaluation

Five-week-old male Institute of Cancer Research (ICR) mice were purchased from Shanghai SLAC Laboratory Animals Co. Ltd. A total of 1×10^6 H22 cells were subcutaneously inoculated into the right flank of ICR mice according to protocols of tumor transplant research, to initiate tumor growth. After incubation for one day, mice were weighted and at random divided into four groups of six animals. The groups treated with **12m** and CA-4 were administered 15, 30 mg/kg in a vehicle of 10% DMF/2% Tween 80/88% saline, respectively. The positive control group was treated with PTX (8 mg/kg) every 2 days by intravenous injection. The negative control group received a vehicle of 10% DMF/2% Tween 80/88% saline through intravenous injection. Treatments of **12m** and CA-4 were done at a frequency of intravenous injection one dose per day for a total 21 consecutive days while the positive group was treated with PTX one dose per two days. The mice were sacrificed after the treatments and the tumors were excised and weighed. The inhibition rate was calculated as follows: Tumor inhibitory ratio (%) = (1-average tumor weight of treated group/average tumor weight of control group) \times 100%.

4.3 Molecular modeling

In our study, the X-ray structure of the DAMA-colchicine- α,β -tubulin complex was downloaded from the Protein Data Bank (PDB code 1SA0). The protein was prepared by removal of the stathmin-like domain, subunits C and D, water molecules and colchicine using Discovery Studio modules. The docking procedure was performed by employing DOCK program in Discovery Studio 3.0 software, and the structural image was obtained using PyMOL software.

Acknowledgments

The authors acknowledge the National Natural Science Foundation of China (No. 81673306, 81703348), and The Open Project of State Key Laboratory of Natural Medicines, China Pharmaceutical University (No. SKLNMKF 201710) for financial support.

Reference

- [1] K. Downing, E. Nogales, Tubulin structure: insights into microtubule properties and functions, *Curr. Opin. Chem. Biol.* 8 (1998) 785-791.
- [2] M. Jordan, L. Wilson, Microtubules as a target for anticancer drugs, *Nat. Rev. Cancer* 4 (2004) 253-265.
- [3] C. Dumontet, M. Jordan, Microtubule-binding agents: a dynamic field of cancer therapeutics, *Nat. Rev. Drug Discov.* 9 (2010) 790-803.
- [4] M. Marx, Small-molecule, tubulin-binding compounds as vascular targeting agents, *Expert Opin. Ther. Pat.* 12 (2002) 769-776.
- [5] M.J. Perez-Perez, E.M. Priego, O. Bueno, M.S. Martins, M.D. Canela, S. Liekens, Blocking blood flow to solid tumors by destabilizing tubulin: An approach to targeting tumor growth, *J. Med. Chem.* 59 (2016) 8685-8711.
- [6] E. Porcù, R. Bortolozzi, G. Basso, G. Viola, Recent advances in vascular disrupting agents in cancer therapy, *Future Med. Chem.* 6 (2014) 1485-1498.
- [7] M. Driowya, J. Leclercq, V. Verones, A. Barczyk, M. Lecoeur, N. Renault, N. Flouquet, A. Ghinet, P. Berthelot, N. Lebegue, Synthesis of triazoloquinazolinone based compounds as tubulin polymerization inhibitors and vascular disrupting agents, *Eur. J. Med. Chem.* 115 (2016) 393-405.
- [8] S. Guggilapu, L. Guntuku, T. Reddy, A. Nagarsenkar, D. Sigalapalli, V.G.M.Naidu, S. K.Bhargava, N. Bathini, Synthesis of thiazole linked indolyl-3-glyoxylamide derivatives as tubulin polymerization inhibitors, *Eur. J. Med. Chem.* 138 (2017) 83-95.
- [9] W. Li, H. Sun, S. Sun, Z. Zhu, J. Xu, Tubulin inhibitors targeting the colchicine binding site: a perspective of privileged structures, *Future med. chem.* 9 (2017) 1765-1794.
- [10] S. Ducki, R. Forrest, J. Hadfield, A. Kendall, N. Lawtence, A. McGowm, D. Rennison, Potent antimetabolic and cell growth inhibitory properties of substituted chalcones, *Bioorg. Med. Chem. Lett.* 8 (1998) 1051-1056.
- [11] N.J. Lawrence, R. P. Patterson, L. Ooi, D. Cook, S. Ducki, Effects of α -substitutions on structure and biological activity of anticancer chalcones, *Bioorg. Med. Chem. Lett.* 16 (2006) 5844-5848.
- [12] S. Ducki, D. Rennison, M. Woo, A. Kendall, J.F. Chabert, A.T. McGowm, N.J. Lawrence, Combretastatin-like chalcones as inhibitors of microtubule polymerization. Part 1: synthesis and biological evaluation of antivasular activity, *Bioorg. Med. Chem.* 17 (2009) 7698-7710.
- [13] D.C. Meadows, J. Gervay-Hague, Vinyl sulfones: synthetic preparations and medicinal chemistry applications, *Med. Res. Rev.* 26 (2006) 793-814.
- [14] J. Palmer, D. Rasnick, J. Klaus, D. Bromme, Vinyl Sulfones as Mechanism-Based Cysteine Protease Inhibitors, *J. Med. Chem.* 38 (1995) 3193-3196.
- [15] S. Woo, J. Kim, M. Moon, S. Han, S. Yeon, J. Choi, B. Jang, H. Song, Y. Kang, J. Kim, J. Lee, D. Kim, O. Hwang, K. Park, Discovery of vinyl sulfones as a novel class of neuroprotective agents toward Parkinson's disease therapy, *J. Med. Chem.* 57 (2014) 1473-1487.

- [16] X. Ning, Y. Guo, X. Wang, X. Ma, C. Tian, X. Shi, R. Zhu, C. Cheng, Y. Du, Z. Ma, Z. Zhang, J. Liu, Design, synthesis, and biological evaluation of (e)-3,4-dihydroxystyryl aralkyl sulfones and sulfoxides as novel multifunctional neuroprotective agents, *J. Med. Chem.* 57 (2014) 4302-4312.
- [17] Y. Shen, C.A. Zifcsak, J. E. Shea, X. Lao, O. Bollt, X. Li, J. G. Lisko, J. P. Theroff, C. L. Scaife, M.A. Ator, B.A. Ruggeri, B.D. Dorsey, S.K. Kuwada, Design, synthesis, and biological evaluation of sulfonyl acrylonitriles as novel inhibitors of cancer metastasis and spread, *J. Med. Chem.* 58 (2015) 1140-1158.
- [18] M. Reddy, M. Mallireddigari, S. Cosenza, V. Pallela, N. Iqbal, K. Robell, A. Kang, E. Reddy, Design, synthesis, and biological evaluation of (E)-styrylbenzylsulfones as novel anticancer agents, *J. Med. Chem.* 51 (2008) 86-100.
- [19] M. V. Reddy, P. Venkatapuram, M. R. Mallireddigari, V. R. Pallela, S. C. Cosenza, K. A. Robell, B. Akula, B. S. Hoffman, E. P. Reddy, Discovery of a clinical stage multi-kinase inhibitor sodium (E)-2-[2-methoxy-5-[(2',4',6'-trimethoxystyrylsulfonyl)methyl]phenylamino]acetate (ON 01910.Na): synthesis, structure-activity relationship, and biological activity, *J. Med. Chem.* 54 (2011) 6254-6276.
- [20] M. V. Reddy, M. R. Mallireddigari, V. R. Pallela, S. C. Cosenza, V. K. Billa, B. Akula, D. R. C. Subbaiah, E. V. Bharathi, A. Padgaonkar, H. Lv, J. M. Gallo, E. P. Reddy, Design, synthesis, and biological evaluation of (E)-N-aryl-2-arylethanesulfonamide analogues as potent and orally bioavailable microtubule-targeted anticancer agents, *J. Med. Chem.* 56 (2013) 5562-5586.
- [21] PR Clarke, LA. Allan, Cell-cycle control in the face of damage – a matter of life or death, *Trends Cell Biol.* 19 (2009) 89–98.
- [22] J Yan, J Chen, S Zhuang, J Hu, L Ling, X Li, Synthesis, evaluation, and mechanism study of novel indole-chalcone derivatives exerting effective antitumor activity through microtubule destabilization in vitro and in vivo, *J. Med. Chem.* 59(2016) 5264-5283.
- [23] H. Chai, K. Hoang, M. Vu, K. Pasunooti, C. Liu, X. Liu, N-Linked Glycosyl Auxiliary-Mediated Native Chemical Ligation on Aspartic Acid: Application towards N-Glycopeptide Synthesis, *Angew. Chem. Int. Ed.* 55 (2016) 10363-10367.

Highlights:

- A series of novel vinyl sulfone and sulfoxide derivatives were synthesized.
- **12m** showed the most potent *in vitro* anti-proliferative activity.
- **12m** was identified as a tubulin polymerization inhibitor with potent vascular disrupting activity.
- **12m** exhibited tumor growth inhibition in H22 liver cancer allograft mouse model.